Toxicon 107 (2015) 163–174

Contents lists available at ScienceDirect

Toxicon

journal homepage: www.elsevier.com/locate/toxicon

Mass spectrometry guided venom profiling and bioactivity screening of the Anatolian Meadow Viper, *Vipera anatolica*

Bayram Göçmen [a, 1], Paul Heiss [b, 1], Daniel Petras [b], Ayse Nalbantsoy [c, *], Roderich D. Süssmuth [b, **]

[a] Zoology Section, Department of Biology, Faculty of Science, Ege University, 35100 Bornova, Izmir, Turkey
[b] Technische Universität Berlin, Institut für Chemie, Strasse des 17. Juni 124, 10623 Berlin, Germany
[c] Department of Bioengineering, Faculty of Engineering, Ege University, Bornova, 35100 Izmir, Turkey

ARTICLE INFO

Article history:
Received 1 August 2015
Received in revised form
27 August 2015
Accepted 10 September 2015
Available online 16 September 2015

Keywords:
Viperidae
Anatolian Meadow Viper
Vipera anatolica
Snake venomics
Top-down venomics
Cytotoxicity
Bioactivity screening

ABSTRACT

This contribution reports on the first characterization of the venom proteome and the bioactivity screening of *Vipera anatolica*, the Anatolian Meadow Viper. The crude venom as well as an isolated dimeric disintegrin showed remarkable cytotoxic activity against glioblastoma cells. Due to the rare occurrence and the small size of this species only little amount of venom was available, which was profiled by means of a combination of bottom-up and top-down mass spectrometry. From this analysis we identified snake venom metalloproteases, cysteine-rich secretory protein isoforms, a metalloprotease inhibitor, several type A2 phospholipases, disintegrins, a snake venom serine protease, a C-type lectin and a Kunitz-type protease inhibitor. Furthermore, we detected several isoforms of above mentioned proteins as well as previously unknown proteins, indicating an extensive complexity of the venom which would have remained undetected with conventional venomic approaches.

1. Introduction

Snake venom, which consists mainly of a mixture of proteins and peptides, has evolved over eons of years to immobilize and kill the prey as fast and as efficient as possible. Snake venoms also cause many human fatalities (>90,000) each year (Casewell et al., 2014). Apart from these terrible consequences of snake envenomation, the toxins also represent an important natural source of potential lead structures for the treatment of various human diseases (Kang et al., 2011; McCleary and Kini, 2013). The medical potential of snake venoms was already known in the ancient world, where it was used in small doses as a traditional medicine (Vetter et al., 2011). Currently there are six FDA-approved drugs on the market which are based on venom toxins (King, 2011) of which the majority originate from snakes. One of the most prominent example is captopril, an lifesaving anti-hypertensive drug derived from a bradykinin potentiating peptide from *Bothrops jararaca* (Ferreira, 1965; Rubin et al., 1978), a pit viper from the tropical and subtropical forests in southern Brazil, Paraguay and the North of Argentina (Goncalves-Machado et al., 2015). Nevertheless, not only for the treatment of cardiovascular diseases snake toxins may be applicable, as there have been reported effects against neuropathic pain (Woolf, 2013) and tumors (Calderon et al., 2014). Particularly non-toxic doses of snake venom have been shown to reduce the size of solid tumors as well as inhibition of tumor angiogenesis (Swenson et al., 2004; Zhou et al., 2000).

In general, snake toxins target a wide range of cellular mechanisms, which are typically neural receptors, the cell membrane and the blood coagulation cascade (Chippaux, 2006). Accordingly, the toxins have been grouped into neurotoxins, cytotoxins and hemotoxins composed of around 10 protein families (three-finger toxins; protease inhibitors; C-type lectins; vascular-, endothelial- and nerve growth factors; cysteine-rich secretory proteins (CRISPs), metallo-proteases (SVMP); serine-proteases (SVSP); L-amino acid oxidases (LAAO); acetylcholine esterases (AChEs) and nucleotidases) as well as peptides resulting from proteolytic cleavage

* Corresponding author.
** Corresponding author.
E-mail addresses: analbantsoy@gmail.com (A. Nalbantsoy), roderich.suessmuth@tu-berlin.de (R.D. Süssmuth).
[1] Both authors contributed equally to this work.

http://dx.doi.org/10.1016/j.toxicon.2015.09.013
0041-0101/

(bradykinin-potentiating peptides, natriuretic peptides, disintegrins and SVMP-inhibitors) (Chippaux, 2006; Fry, 2015).

Over the past decades, the analytical characterization of venom has been continuously enhanced by technological developments. The implementation of mass spectrometric techniques into proteomic workflows as well as next-generation sequencing, have advanced the analysis of snake venoms significantly. Since venom research evolved mainly from hypothesis-driven approaches, focused on single toxins, to a systematic, untargeted analysis, several so-called "bottom-up" approaches have been developed (Calvete, 2014). These techniques typically include a proteolytic digestion of the proteins to facilitate their analysis and identification (Calvete, 2013). The digestion step however multiplies the number of molecules present in a sample and disconnect structural relation within highly homologous isoforms and eventually occurring post-translational modified proteins. To overcome the sample complexation and loss of information by protease digestion we recently introduced a top-down mass spectrometric approach in an exemplary study of King Cobra venom (Petras et al., 2015). However, even equipped with a set of toolboxes, including high throughput techniques capable of a rapid and systematic venom analysis, only few venoms from over 600 biomedically relevant snake species have been thoroughly studied (Brahma et al., 2015; Calvete, 2013). Furthermore, most of these studies only reflect a partial picture of the whole-venom of a certain snake species, since toxin structures and venom composition show considerable intraspecific and geographic variability (Casewell et al., 2014; Reyes-Velasco et al., 2015; Vonk et al., 2013).

The distribution of poisonous snakes in Turkey includes three families: *Colubridae*, *Viperidae* and *Elapidae*. Particularly, viper species are quite abundant and some species are endemic (Göçmen et al., 2006a). The Anatolian Meadow Viper, *Vipera anatolica*, which was first recognized as a differentiated taxon among the Euro-Asiatic vipers in 1983 (Böhme and Joger, 1983) can only be found in a narrow and limited area near Elmali, in the Antalya province (Göçmen et al., 2014). To the best of our knowledge, no studies on the venom composition of *V. anatolica* have been reported in literature so far. Thus, *V. anatolica* venom might be a source of untapped bioactive peptides and proteins with interesting pharmacological properties. As a part of our ongoing research on snake venoms from Turkish species, the purpose of this work was to profiling *V. anatolica* venom composition and to assess potential cytotoxic activities against different cancer cell lines.

2. Material and methods

2.1. Collection and preparation of venom samples

The study was approved by the Ege University, Local Ethical Committee of Animal Experiment (Number: 2010/43) and a special permission (2011/7110) for field studies was accepted from the Republic of Turkey, Ministry of Forestry and Water Affairs. All specimens were released back into their natural environment after investigation.

V. anatolica individuals were collected from late April to mid-October 2014 in Cıglıkara forests, North West of Kohu Mt. in Elmalı, Antalya provinces in Turkey, in altitudes between 1650 and 1750 m (MASL). Crude *V. anatolica* venom was extracted from two male and one female adult, using a paraffin-covered laboratory beaker without exerting pressure on the venom glands. Venom samples were pooled in one tube and centrifuged at 2000 × g for 10 min at +4 °C to remove cell debris. Supernatants were collected, immediately frozen at −80 °C, and then lyophilized. Lyophilized samples were stored at 4 °C.

2.2. Determination of protein concentration

Protein concentration was determined from diluted venom sample (4 mg/mL) in deionized water by Bradford assay(Bradford, 1976) using a UV/Vis spectrophotometer (VersaMax, Molecular Devices, CA, USA) at a wavelength of $\lambda = 595$ nm. Bovine serum albumin was used as a reference.

2.3. Cell culture and in vitro cytotoxicity assay

The following cell lines were used for determination of cytotoxicity: HeLa (human cervix adenocarcinoma), A-549 (human alveolar adenocarcinoma), MCF-7 (human breast adenocarcinoma), CACO-2 (human colon colorectal adenocarcinoma), mPANC96 (human pancreas adenocarcinoma), PC-3 (human prostate adenocarcinoma), U87MG (human glioblastoma-astrocytoma) cancer cells and as a non-cancerous cell lines, HEK (human embryonic kidney). Cell lines were purchased from ATCC (Manassas, VA, USA). The PC3 cell line was obtained from Dr. K. Korkmaz (Ege University, Bioengineering Department, Bornova-Izmir, Turkey). All cells were cultivated in Dulbecco's modified Eagle's medium F12 (DMEM/F12), supplemented with 10% fetal bovine serum (FBS), 2 mM/L glutamine, 100 U/mL of penicillin and 100 μg/mL of streptomycin (Lonza, Visp, Switzerland). The cells were incubated at 37 °C in a humidified atmosphere of 5% CO_2.

Cytotoxicity of crude venom was determined by following the general procedure based on cell viability using a modified colorimetric MTT [3-(4,5-dimethyl-2-thiazolyl)-2,5-diphenyl-2H-tetrazolium bromide)] assay (Mosmann, 1983; Yalcin et al., 2014). The optical density (OD) was measured in triplicates at $\lambda = 570$ nm (with a reference wavelength $\lambda = 690$ nm) by UV/Vis spectrophotometry (Thermo, Bremen, Germany). All cell lines were cultivated for 24 h in 96-well microplates with an initial concentration of 1×10^5 cells/mL. Subsequently, the cultured cells were treated with different doses of venom and incubated for 48 h at 37 °C. The plant-derived compound parthenolide (a sesquiterpene lactone) was used as a positive cytotoxic control agent. Percentages of surviving cells in each culture were determined after incubation with venom. The viability (%) was determined by the following formula:

%Viable cells = [(absorbance of treated cells)−(absorbance of blank)]/[(absorbance of control)−(absorbance of blank)] × 100

2.4. Determination of half maximal inhibitory concentration (IC_{50})

In cell culture studies for untreated cell lines (negative controls) cytotoxicity was set to 0%. The IC_{50} values were calculated by fitting the data to a sigmoidal curve and using a four parameter logistic model and presented as an average of three independent measurements. The IC_{50} values were reported at 95% confidence interval and calculations were performed using Prism 5 software (GraphPad5, San Diego, CA, USA). The values of the blank wells were subtracted from each well of treated and control cells and half maximal inhibition of growth (IC_{50}) were calculated in comparison to untreated controls.

2.5. Morphological studies

The morphological studies of the cells were performed with an inverted microscope (Olympus, Tokyo, Japan) compared to the control group 48 h after treatment.

2.6. Preparation of venom samples for proteomic analysis

For LC-MS analysis and semi-preparative HPLC fractionation, crude venom was dissolved in aqueous 1% formic acid (HFo) (v/v) to a final concentration of 10 mg/mL, and centrifuged at 20,000 g for 5 min. For top-down measurements disulfide bonds were reduced. Therefore 10 μL of venom (10 mg/mL) was mixed with 10 μL of tris(2-carboxyethyl)phosphine (TCEP, 0.5 M) and 30 μL of citrate buffer (0.1 M, pH 3), after which the reaction mixture was incubated for 30 min at 65 °C. Thereafter, the sample was mixed with an equal volume of 1% formic acid and centrifuged at 20,000 × g for 5 min. Then 10 μL of both reduced and non-reduced samples were submitted to top-down measurements. A volume of 100 μL of non-reduced venom was subjected for semi-preparative HPLC fractionation.

2.7. Top-down venomics

LC-ESI-HR-MS/MS experiments were performed on an LTQ Orbitrap XL mass spectrometer (Thermo, Bremen, Germany) coupled to an Agilent 1260 HPLC system (Agilent, Waldbronn, Germany). A Suppelco Discovery 300 Å C18 (2 × 150 mm, 3 μm particle size) column was used. Typically the flow rate was set to 0.3 mL/min and a gradient of 0.1% HFo in water (solution A) and 0.1% HFo in acetonitrile (ACN) (solution B) was used. The gradient started isocratically (5% B) for 1 min, followed by an increase from 5 to 40% B over 40 min, 40–70% over 20 min, a washout at 70% B for 10 min, and a re-equilibration phase at 5% B. ESI settings were 40 L/min sheath gas; 20 L/min auxiliary gas; spray voltage, 4.8 kV; capillary voltage, 46 V; tube lens voltage, 135 V and capillary temperature, 330 °C. For information dependent acquisition (IDA), four scan events were set with 2 micro scans and 500 ms maximal fill time. The survey scan was performed with mass resolution R = 100,000 (at m/z 400). For MS/MS R was set to 60,000 (at m/z 400). Every cycle contained two CID scans of the two most abundant ions of the survey scan. Normalized collision energy was set to 35% for CID. The default charge state was set to 8 + and the activation time to 30 msec. The precursor selection window was set to 2 m/z. Dynamic exclusion was performed with a 3 m/z exclusion window for precursor ions with 1 repeat within 10 s. The exclusion list contained maximal 50 ions for a duration of 20 s. For the deconvolution of isotopically resolved spectra the XTRACT algorithm of Xcalibur (Thermo, Bremen, Germany) was used. For isotopically not resolved spectra the Zscore algorithm (Zhang and Marshall, 1998) implemented in the magic transformer (MagTran) tool was used for charge distribution deconvolution. For protein identifications, deconvoluted mass spectra were analyzed manually. The resulting *de novo* generated sequence tags were BLASTed against the NCBI non-redundant Viperidae database (http://blast.ncbi.nlm.nih.gov/Blast.cgi) using the BLASTP algorithm (Altschul et al., 1990).

2.8. Bottom-up venomics

For bottom-up analysis, the venom was dissolved to a concentration of 10 mg/mL in aqueous 1% HFo and 5% acetonitrile (ACN). A volume of 100 μL was subjected to semipreparative reverse-phase (RP) HPLC separation on a Suppelco Discovery 300 Å C18 (4.6 × 150 mm, 3 μm particle size) column. The flow rate was set to 1 mL/min. A linear gradient of 0.1% HFo in water (solution A) and 0.1% HFo in ACN (solution B), isocratically (5% B) for 5 min, followed by linear gradients of 5–40% B for 95 min, 40–70% for 20 min, 70% B for 10 min, and finally re-equilibration at 5% B for 10 min was used. Peak detection was performed at λ = 214 nm using a diode array detector (DAD). Chromatographic fractions were collected manually, dried in a vacuum centrifuge, chemically reduced with dithiothreitol (DTT) and submitted to SDS-PAGE. Subsequent Coomassie stained bands were excised from the gel and subjected to in-gel reduction (10 mM DTT in 25 mM $(NH_4)HCO_3$, pH 8.3, for 45 min at 65 °C) and alkylation (50 mM iodacetamide in 50 mM $(NH_4)HCO_3$, pH 8.3, for 30 min at 25 °C), followed by in-gel trypsin digestion (12 h at 37 °C with 66 ng sequencing-grade trypsin/mL in 25 mM $(NH_4)HCO_3$, 10% ACN; 0.25 mg/sample). Tryptic peptides were dried in a vacuum centrifuge, re-dissolved in 15 mL of 5% ACN containing 0.1% HFo, and submitted to LC-MS/MS analysis using a an Orbitrap XL hybrid mass spectrometer (Thermo, Bremen, Germany) equipped with an HPLC system (Agilent, Waldbronn, Germany). LC separation was performed on a Grace Vydac 218MSC18 column (2.1 × 15 mm, 5 μm) with a flow rate of 0.3 mL/min. A gradient was applied using of 0.1% HFo in water (solution A) and in ACN (solution B). The gradient started isocratically with 5% B for 2 min, followed by an increase over 10 min from 5 to 40% B, 40–99% B over 15 min, and held at 99% B for 5 min with final re-equilibration phase at 5% B for 5 min. MS experiments were performed in the Orbitrap analyser with R = 15,000at m/z 400 and maximum filling time of 200 ms for both survey and first product ion scans. MS/MS fragmentation of the two most intense ions was performed in the LTQ using CID (30 ms activation time); the collision energy was set to 35%. Precursor-ion isolation was performed within a mass window of 2 m/z. Dynamic exclusion was set up for a 3 m/z windows for up to 50 precursor ions with a repeat of 2 within 30 s. *De novo* annotation of MSMS spectra was performed with the DeNovoGUI tool (Muth et al., 2014). Manually proved sequence tags were searched against a Viperidae non-redundant protein database of UniProtKB/TrEMBL using BLASTP (Altschul et al., 1990).

2.9. Relative toxin quantification

The relative abundances (percentage of the total venom proteins) of the different protein families were calculated as the ratio of the sum of the areas of the reverse-phase UV_{214}-chromatographic peaks containing proteins from the same family to the total area of venom protein peaks in the reverse-phase chromatogram according to Calvete et al. (Calvete, 2014). If more than one protein was present in a reverse-phase fraction, their proportions were estimated by the relative abundance of deconvoluted top-down spectra. If co-eluting proteins were observed by SDS-PAGE which were not accessible by mass spectrometry, their relative abundance was estimated by optical signal strength of the Coomassie-stained bands (Goncalves-Machado et al., 2015).

3. Results and discussion

3.1. Vipera anatolica

The Anatolian Meadow Viper is an viper species endemic in an area less than 100 km^2 east of Elmali, in Southwestern Anatolia, Turkey (shown in Fig. 1B). The species is extremely rare and listed as critically endangered on the IUNC Redlist 2015 (Varol Tok et al., 2015). It took us several years and expeditions to finally capture three individuals (2 male and 1 female) in lengths between 20 and 40 cm. Fig. 1 A shows a photograph of a female and a male individual in their natural habitat. Venom of each individual was extracted twice and freeze dried, which yielded a total amount of ~1 mg dried venom. The peptide and protein concentration was determined by means of a Bradford assay as ~38% (wt%).

In order to obtain a detailed picture of the venom composition and to assess the cytotoxicity of isolated toxins we performed a detailed proteomic analysis and fractionation of the venom. It is important to note that the limited access to the snakes, due to their

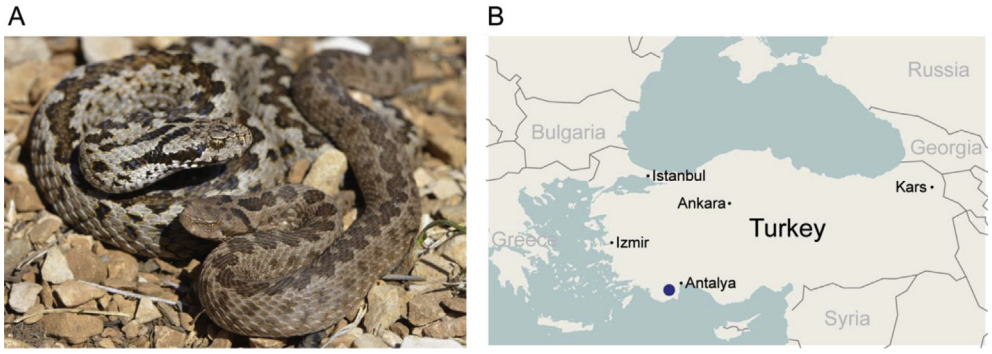

Fig. 1. A: Photograph of *Vipera anatolica* – The photo was taken during a fieldtrip in October 2014 at Kohu Mt., Elmali, Antalya, Turkey. The individual on the right is an adult female; the second individual is an adult male. B: Geographic distribution of *Vipera anatolica*. The Anatolian Meadow Viper is an endemic viper species in an area less than 100 km^2 east of Elmali, in southwestern Anatolia, Turkey, blue circle. (For interpretation of the references to colour in this figure legend, the reader is referred to the web version of this article.)

low abundance and the minimal amounts of venom available for mass spectrometric analysis, made a classic venomic protocol (HPLC fractionation, SDS-PAGE, in gel trypsin digestion followed by MSMS *de novo* sequencing) aiming at a thorough proteomic characterization an extremely challenging task (Calvete, 2013, 2014; Goncalves-Machado et al., 2015). This is exemplified by the fact that the typical amount of venom applied to one semi-preparative HPLC run equals the amount of venom we had available to perform the complete analytical characterization. In order to obtain a general overview of the molecular masses of the venom components, including low abundant and low molecular mass compounds which might not be gathered during SDS-PAGE, we thus decided to perform an initial top-down mass spectrometric analysis of the crude venom.

3.2. Top-down venomics

In top-down approaches the proteins are not digested prior to mass spectrometric analysis (Ge et al., 2002). Instead they are directly ionized and thus render the molecular mass of the intact protein. Ideally, if the protein is further fragmented in the gas phase, amino acid sequences and site specific modifications can be determined. Therefore isotope resolution is typically required, in order to deconvolute the complex fragment spectra. This is limited by the resolution provided by the mass analyzer used, typically <50 kDa for Orbitrap analyzers with R = 100,000 at 400 m/z. As the majority of the toxins present in viper venoms exceed this molecular weight (>50 kDa, SVMPs, SVSPs, LAAOs etc.), one can still make use of deconvolution based on charge distribution of protein MS1 spectra.

An inherent limitation of SDS-PAGE is that small sized peptides and proteins are not efficiently resolved which makes a direct HPLC-supported mass spectrometric analysis the most effective way to gather structural information (Petras et al., 2015). In Fig. 2 the UV chromatogram of the semi-preparative fractionation and the corresponding Coomassie-stained SDS-PAGE analysis of the fractions as well as the total ion current (TIC) of the LCMS analysis of native venom is shown. Due to the difference in column size the retention times are slightly shifted between the LCMS analysis and the semiprep-HPLC run. In the initial top-down mass profiling ~100 toxin masses were detected which are listed in Table 1 (All deconvoluted mass spectra are shown in the supplemental information). In total we observed 22 molecular masses <1 kDa and 53 molecular masses between 1 and 9 kDa, which represents ~75% of the peptide and protein species. Furthermore the initial top-down analysis rendered another 27 compounds between 9 and 60 kDa. Interestingly, the majority of venom toxins seem to consist of molecular masses in the low mass range (<9 kDa) which, at the same time occur in low concentrations.

In order to obtain useful fragment spectra of toxins in subsequent MS2 experiments it was required to reduce potentially occurring disulfide bridges of toxins prior to top-down analysis. We thus reduced the venom chemically using TCEP prior to a second LCMS run with data dependent MS2 acquisition. Because a comprehensive analysis of top-down data relies strongly on the availability of transcriptome and/or genome data, which yet does not exist for *V. anatolica* and is still limited for closely related Viperidae, we manually analyzed the ESI mass spectra and searched *de novo* generated sequence tags against a *Viperidae* database using the Blast algorithm. Using this method we could identify a PLA_2 fragment with the sequence tag (1871)ALFSYSDYGCYCGWG(1931). As the spectrum was obtained from chemically reduced venom the observed fragmentation of the PLA2 could have occurred during the sample preparation before mass spectrometric analysis. Furthermore we could directly identify a disintegrin like compound with the sequence tag (5085)-DYCTGJS-(221). Fig. 3 exemplarily shows the deconvoluted top-down MS1 and MS2 spectra of the disintegrin-like venom protein with a molecular weight of 6047.5 Da (peak 11 in Fig. 2). In the top-down MS analysis the non-reduced disintegrin like compounds (peak 11) instead showed average molecular masses of 13,982.8, 14,001.7 and 14,017.7 Da which correspond to the SDS-PAGE analysis of the isolated peak with a band height at ~ 14 kDa and thus indicates that the disintegrin in peak 11 is a hetero-dimer. Furthermore peak 4 (see Fig. 2) could be identified as a snake venom metalloprotease inhibitor, which is commonly present in *Viperidae* venoms (Munekiyo and Mackessy, 2005; Wagstaff et al., 2008). Nevertheless, through the difficulties in ionizing and deconvoluting high molecular mass components (>50 kDa) which represent the majority of the *V. anatolica* venom content, the peptide/protein IDs obtained from the initial top-down analysis are limited. A future solution to increase the number of protein IDs obtained by top-down MS/MS would be a pre-fractionation by size exclusion chromatography and thus an enrichment of the low abundant low molecular mass toxins, which are accessible for top-down MS/MS elucidation but remained unselected during the IDA MS/MS experiments. A further general improvement for the venom proteome analysis would be a transcriptome analysis of *V. anatolica* venom gland tissue, which would enable the use of spectra-database comparisons for data analysis, which is more effective than the generation of *de novo* sequence tags and a subsequent Blast search.

3.3. Bottom-up venomics

Besides the initial top-down mass spectrometric characterization rendering intact venom components, which already showed a

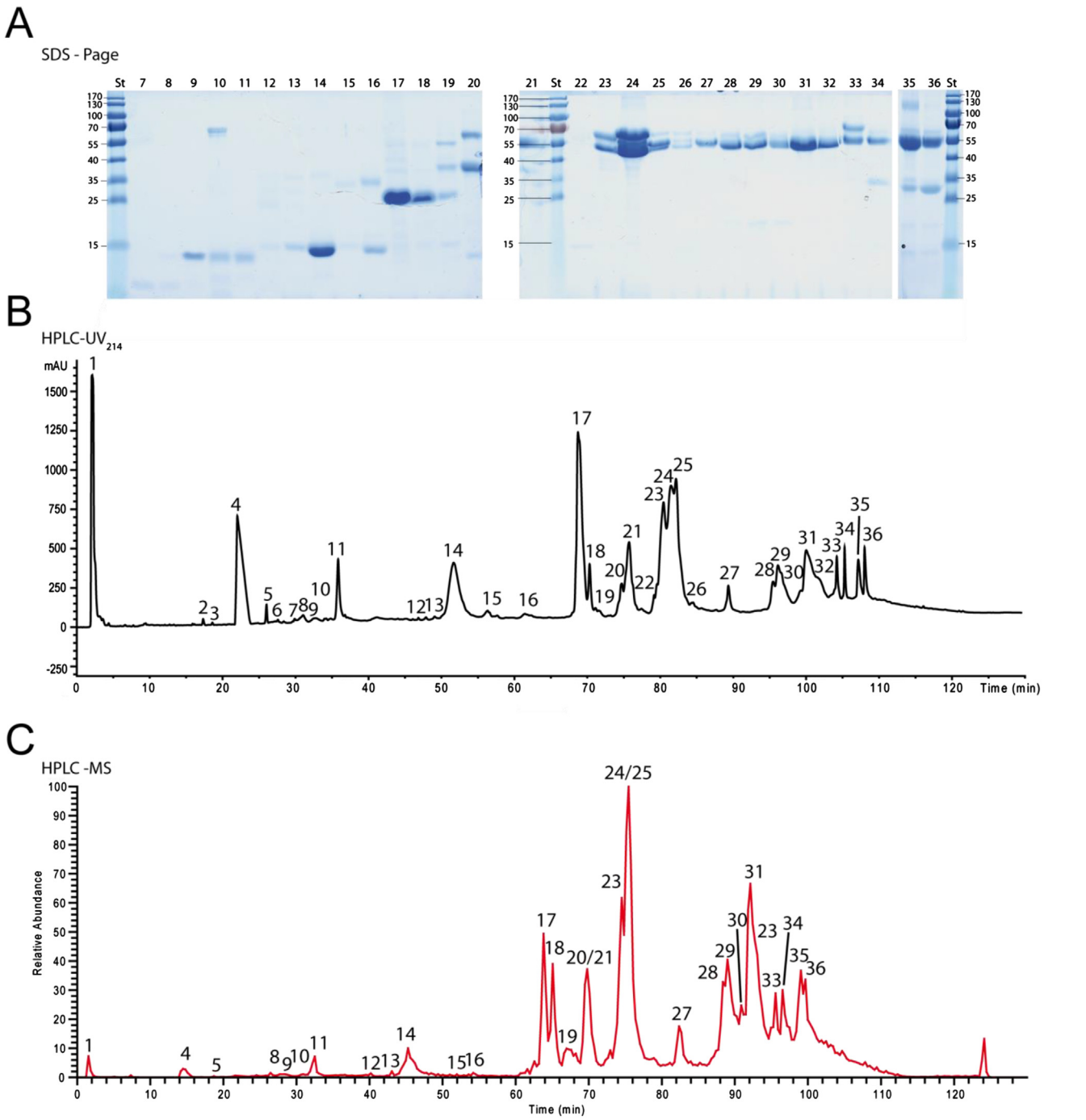

Fig. 2. Venom profile of *Vipera anatolica*. Reverse-phase HPLC separation of *V. anatolica* venom proteins. A shows the SDS-PAGE analysis of fractions collected from the semi-preparative HPLC run displayed in B. Excised protein bands were identified by bottom-up *de novo* sequencing. Panel C shows the top-down MS1 analysis. [Molecular masses, sequence tags and database hits are listed in Table 2. Extracted and deconvoluted mass spectra are shown in the supplemental material. The deconvoluted MS1 and MS2 spectra of peak 11 are shown in Fig. 4].

detailed picture of the structural diversity of the venom, we identified the remaining toxin families through the application of a bottom-up approach. By means of HPLC fractionation, SDS-PAGE separation followed by in-gel digestion and LC-MS/MS analysis we could generate 46 *de novo* sequence tags (Table 1), representing seven toxin families. The percentage of the venom protein content is presented in the pie chart in Fig. 4. For determination of relative abundance (in %) of venom proteins the intensities of UV peak areas were used. In case of coelution the relative intensity of deconvoluted top-down spectra of proteins was taken as a measure. If an inefficient ionization of proteins was observed the signal strength of SDS-PAGE bands served as a measure. Hence, the most abundant toxin family is represented by snake venom metalloproteases (SVMP, 41.5%), followed by two cysteine-rich secretory protein isoforms (CRISP, 15.9%) with molecular masses of 24,645.0 Da and 24,544.1 Da, metalloprotease inhibitor (SVMPi, 9.3%), A_2 phospholipases (PLA2, 8.1%), disintegrins (2.0%), a snake venom serine protease (SVSP, 1.6%), a C-type lectin (1.1%) and a

Table 1
Venom peptides and proteins identified from *Vipera anatolica*. Protein assignment of RP-HPLC fractions (Fig. 4) by LCMS and MS/MS analysis. Peak numbering corresponds to the UV and MS chromatograms shown in Fig. 2. Sequence tags are obtained by *de novo* analysis of intact protein and tryptic peptide MS/MS spectra. Protein IDs are obtained by BLASTP analysis of the sequence tags against a viperid non-redundant protein database. Molecular weight was determined by SDS-PAGE (*) and top-down MS analysis (#) and are shown as average masses.

Peak number	Identified sequence tag	Protein ID	Blast E-value	NCBI accession number	M [kDa]*	M [Da]#	Method
1		unknown (~peptide)				429.0; 621.0; 835.1; 1071.0; 1241.1	Top-down MS1
2		unknown (~peptide)				579.2; 816.4; 1269.6; 1600.8; 2049.0	Top-down MS1
3		unknown (~peptide)				969.4; 1026.5	Top-down MS1
4	pQKW	Metalloprotease inhibitor				443.2	De novo from Top-down MS2
5		unknown (~peptide)				474.2; 598.4; 752.4; 858.3; 1128.6; 1747.7	Top-down MS1
6		unknown (~peptide)				454.3; 499.4; 726.8	Top-down MS1
7		unknown (~peptide)				452.3; 606.3	Top-down MS1
8		unknown (~peptide)				808.4; 1128.6; 3943.8	Top-down MS1
9	(423.02)-YGGCGGNANNFK-COOH	~Kunitz-type serine protease inhibitor	2.0E-08	P0DKL8.1	14	6737.9	De novo from Trypsin-digest, Top-down MS1, Mass from SDS-Page
		unknown (~peptide)				452.3; 497.4; 707.4; 781.4; 3137.5; 4014.8; 4848.2; 5123.4	Top-down MS1
10		unknown (~Protein)			14; 56		Mass from SDS-Page
		unknown (~peptide)				1115.6; 3119.5; 3233.5	Top-down MS1
11	NH2-FJNAGTJCQY-(227.02)	~Disintegrin VA6	3.0E-04	P0C6A5.1	14	13,982.8; 14,001.7; 14,017.7	De novo from Trypsin-digest, Top-down MS1, Mass from SDS-Page
	(532.05)-DYCDGJSSDGVDR-COOH	~Disintegrin VB7A	2.0E-02	P0C6A6.1			
	(1001.56)-YQTGJSSDCPR-COOH	~Disintegrin VB7B	6.0E-04	P0C6A7.1			
	(5085)-DYCTGJS-(221)	~Disintegrin VB7A	1.2E-02			6047.5 (reduced)	De novo from Top-down MS2
12		unknown (~peptide)			14	1457.7; 6817.2	Top-down MS1; Mass from SDS-Page
13		unknown (~peptide)			14		Mass from SDS-Page
		unknown (~peptide)				1101.5; 1357.7; 6965.2; 7001.2; 7227.1	Top-down MS1
14	(241.03)-JCFGDQJNTYDK-COOH	~Neutral phospholipase	1.0E-05	P34180.2	14	13,639.9 (5461.6)	De novo from Trypsin-digest,
	(1871)ALFSYSDYGCYCGWG(1931).	A2 ammodytin I2	7.0E-12	CAE47236.1			Top-down MS1,
		~ammodytin I2(C) isoform					Top-down MS2,Mass from SDS-Page
		unknown (~Protein)				6948.3; 6982.2	Top-down MS1
15		unknown (~Protein)				7175.4; 7212.4; 7293.5	Top-down MS1
16a		unknown (~Protein)			35		Mass from SDS-Page
16b	(890.35)-VAAJCFGENJNS-(548.34)	~Neutral phospholipase A2 ammodytin I2	5.0E-06	P34180.2	14	13,637.9	De novo from Trypsin-digest, Top-down MS1, Mass from SDS-Page
	(354.21)-CFGENJNTYDKK-COOH	~Neutral phospholipase A2 ammodytin I2	5.0E-09	P34180.2	14	7276.4; 7903.7	De novo from Trypsin-digest, Top-down MS1, Mass from SDS-Page
		unknown (~Protein)				3772.2; 5549.1; 5586.1; 5677.2; 5713.1	Top-down MS1
17	NH2-SVNPTASNMJK-COOH	~Cysteine-rich venom protein	5.0E-07	B7FDI0.1	25	24,645.0	De novo from Trypsin-digest, Top-down MS1, Mass from SDS-Page
	NH2-SVDFDSESPR-COOH	~Cysteine-rich venom protein	3.0E-05	B7FDI0.1			
	NH2-FJDAYPEAAANAER-COOH	~Cysteine-rich venom protein	7.0E-06	B7FDI0.1			
	(225.09)-EJQNEEPDJHNSJR-COOH	~Cysteine-rich venom protein	2.0E-05	B7FDI0.1			
18	(439.24)-ECGENJYMSTSEVK-COOH	~Cysteine-rich venom protein	1.0E-05	B7FDI0.1	25	24,544.1	De novo from Trypsin-digest, Top-down MS1, Mass from SDS-Page
19a	NH2-AYJGTMCQPK-COOH	~H3 metalloproteinase precursor 1	1.2E-02	AGL45259.1	55	46,397.0	De novo from Trypsin-digest, Top-down MS1, Mass from SDS-Page
19b		unknown (~Protein)			35		Mass from SDS-Page
19c	(186.09)-DFTTESPR-COOH	~Cysteine-rich venom protein	8.6E-02	B7FDI0.1	25		De novo from Trypsin-digest, Top-down MS1, Mass from SDS-Page
19		unknown (~Protein)				1375.8; 6067.3; 6166.3	Top-down MS1
20a		unknown (~Protein)			60		Mass from SDS-Page

20b	NH2-JQGJVSWGS-(487.26)	~Snake venom serine protease nikobin	5.0E-05	E5AJX2.1	35		De novo from Trypsin-digest, Top-down MS1, Mass from SDS-Page
	NH2-JMGWGTJTTTK-COOH	~Snake venom serine protease nikobin	4.5E-02	E5AJX2.1			
	(699.24)-JJJEEWVJDQR-COOH	~Snake venom serine protease nikobin	8.9E-01	E5AJX2.1			
	NH2-FPNGDJKDLMJJR-COOH	~Snake venom serine protease nikobin	4.4E-01	E5AJX2.1			
20c	(1350.51)-JVCDGGDDPGTR-COOH	~ammodytin I1(A) variant (PLA2)	9.5E-02	CAE47176.1	14		De novo from Trypsin-digest, Mass from SDS-Page
21	NH2-TAJDFDGSVJGK-COOH	~metalloproteinase	5.7E-01	ADI47580.1	55		De novo from Trypsin-digest, Mass from SDS-Page
20/21		unknown (~Protein)				3181.2; 4688.4; 5505.0: 7376.8; 7833.8; 12,891.8	Top-down MS1
22		unknown (~Protein)				8172.7; 16,346.4, 16,397.1	Top-down MS1
23a + 24a	NH2-SSDJGFEDYSQJDR-COOH	~Zinc metalloproteinase -disintegrin-like ammodytagin	7.6E-01	P0DJE2.3	70		De novo from Trypsin-digest, Mass from SDS-Page
	(895.05)-JJTFDDSFGEWR-COOH	~Zinc metalloproteinase -disintegrin-like ammodytagin	5.3E-01	P0DJE2.3			
	NH2-JPECJJNKPJR-COOH	~Zinc metalloproteinase -disintegrin-like ammodytagin	4.4E-01	P0DJE2.3			
24b + 25	(373.93)-GDDTJDSFGEWR-COOH	~metalloproteinase F1	8.0E-05	AJC52543.1	60		De novo from Trypsin-digest, Mass from SDS-Page
	NH2-YDYSEDPDYGFGD-(449.1)	~Zinc metalloproteinase -disintegrin-like ammodytagin	1.6E-01	P0DJE2.3			
	NH2-VNJJNEMYJPLNJR-COOH	~H3 metalloproteinase	2.6E-01	AGL45259.1			
23b + 24c	NH2-VPJVGVEJWDHGDJJK-COOH	~H3 metalloproteinase	4.0E-03	AGL45259.1	45	48,693.0	De novo from Trypsin-digest, Mass from SDS-Page, Top-down MS1
	NH2-VNJJNEFYLPJNJR-COOH	~H3 metalloproteinase	3.7E-01	AGL45259.1			
	(174.31)-NJFGEDYSQJDR-COOH	~H3 metalloproteinase	1.5E-02	AGL45259.1			
23–25		unknown (~Protein)				4452.7; 6299.4; 10,102.4; 11,831.3; 24,411.4	Top-down MS1
26	NH2-VPJVGVEJWDVPJTPR-COOH	~metalloproteinase H4-A	2.2E-02	AHB62069.1			De novo from Trypsin-digest
26		unknown (~Protein)				8594.1; 16,106.5	Top-down MS1
27		unknown (~Protein)			50		Mass from SDS-Page
		unknown (~Protein)				6433.0; 9356.4; 16,586.1	TIC Top-down MS1
29b − 30b	NH2-TWFNJNCEER-COOH	~C-type lectin	1.0E-04	Q696W1.1	20	21,892.7	De novo from Trypsin-digest, Top-down MS1, Mass from SDS-Page
28–29		unknown (~Protein)			50	49,184; 24,561.5	TIC Top-down MS1, Mass from SDS-Page
30a		unknown (~Protein)				48,281;	TIC Top-down MS1
30–32		unknown (~Protein)				27,058.0	TIC Top-down MS1
31	(388.99)-PDDPDYGFVDJGTK-COOH	~Zinc metalloproteinase -disintegrin-like ammodytagin	1.0E-08	P0DJE2.3	50		De novo from Trypsin-digest, Mass from SDS-Page
	NH2-TLGJAPVSGMCQPK-COOH	~metalloproteinase H4-A	3.0E-06	AHB62069.1			
	NH2-HDNAQJJTGJDJN-(213.07)	~metalloproteinase H4-A	7.0E-08	AHB62069.1			
32	NH2-MTJEGFJTGLDJNGR-COOH	~Zinc metalloproteinase -disintegrin-like ammodytagin	2.1E-01	P0DJE2.3	50		De novo from Trypsin-digest, Mass from SDS-Page
	NH2-DVGJAPVSGMCQPK-COOH	~metalloproteinase H4-A	2.0E-04	AHB62069.1			
	(323.01)-ATSEQQR-COOH	~metalloproteinase H4-A	1.1E-01	AHB62069.1			
33a	(260.16)-DHJDJJCJJNQPJR-COOH	~Zinc metalloproteinase -disintegrin jararin	1.5E-02	Q0NZX6.1	65	32,076.0	De novo from Trypsin-digest, Mass from SDS-Page, Top-down MS1
	(626.8)-NPESSJJNQPJR-COOH	~metalloproteinase	1.6E-01	ADI47709.1			
33b	NH2-HDNAQJJTGJD-(440.24)	~Zinc metalloproteinase -disintegrin BlatH1	8.0E-05	U5PZ28.1	50	57,085.0	De novo from Trypsin-digest, Mass from SDS-Page, Top-down MS1
	NH2-VTSSGDDTJDSFGEGER-COOH	~metalloproteinase	5.0E-07	ADI47715.1			
	NH2-YYJNEMYJPJNJR-COOH	~metalloproteinase	2.0E-05	ADI47590.1			
34a		unknown (~Protein)			60	26,398.0	TIC Top-down MS1, Mass from SDS-Page
34b		unknown (~Protein)			35	27,603.0	TIC Top-down MS1, Mass from SDS-Page
35a	(493.29)-VSWGSCAQK-COOH		6.6E-02	Q58G94.1	170		De novo from Trypsin-digest

(continued on next page)

Table 1 (*continued*)

		~Thrombin-like enzyme gyroxin B2.1					
35b + 36a	NH2-JJEWSER-COOH	~metalloproteinase F1	1.7E-02	AJC52543.1	50	25,225.0	De novo from Trypsin-digest, Mass from SDS-Page, Top-down MS1
	(37.19)-QJYYTPR-COOH	~H3 metalloproteinase	7.0E-03	AGL45259.1			
	(339.04)-JTPEEKR-COOH	~H3 metalloproteinase	4.9E-01	AGL45259.1			
36a		unknown (~Protein)			27		TIC Top-down MS1, Mass from SDS-Page
36b		unknown (~Protein)					TIC Top-down MS1, Mass from SDS-Page

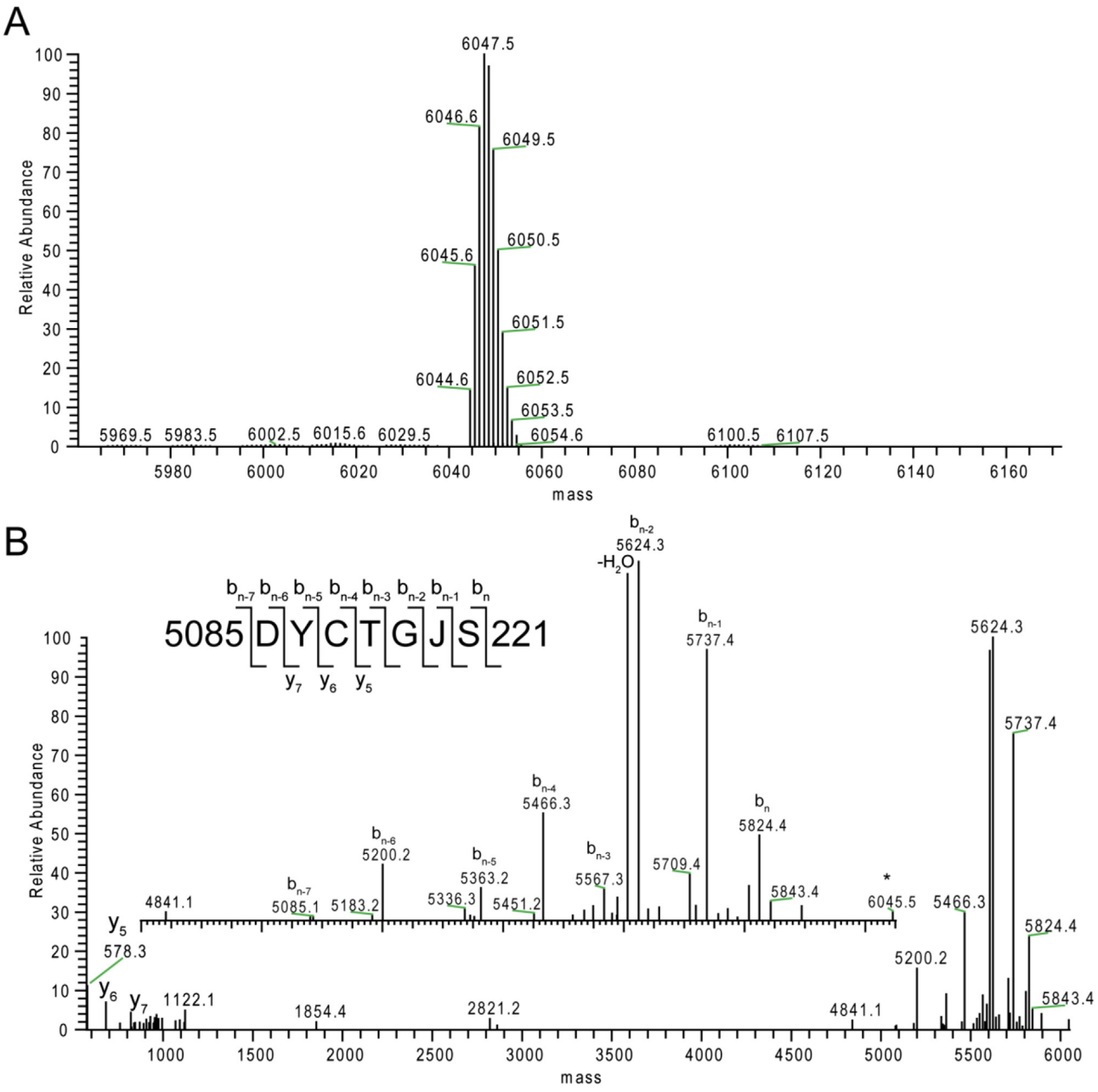

Fig. 3. Top-down spectrum of chemically reduced peak 11, a disintegrin-like venom compound. Panel A shows the deconvoluted MS1 spectrum of peak 11 with a molecular mass of 6047.5 Da (average mass). In B the deconvoluted MS spectra of the 7 times charged precursor (864.94 m/z) is shown. In the low mass range the y-ions and in the high mass zoom the b-ion series is annotated, the resulting sequence tag is displayed above (J stands for either I or L). The resulting database hit is shown in Table 2.

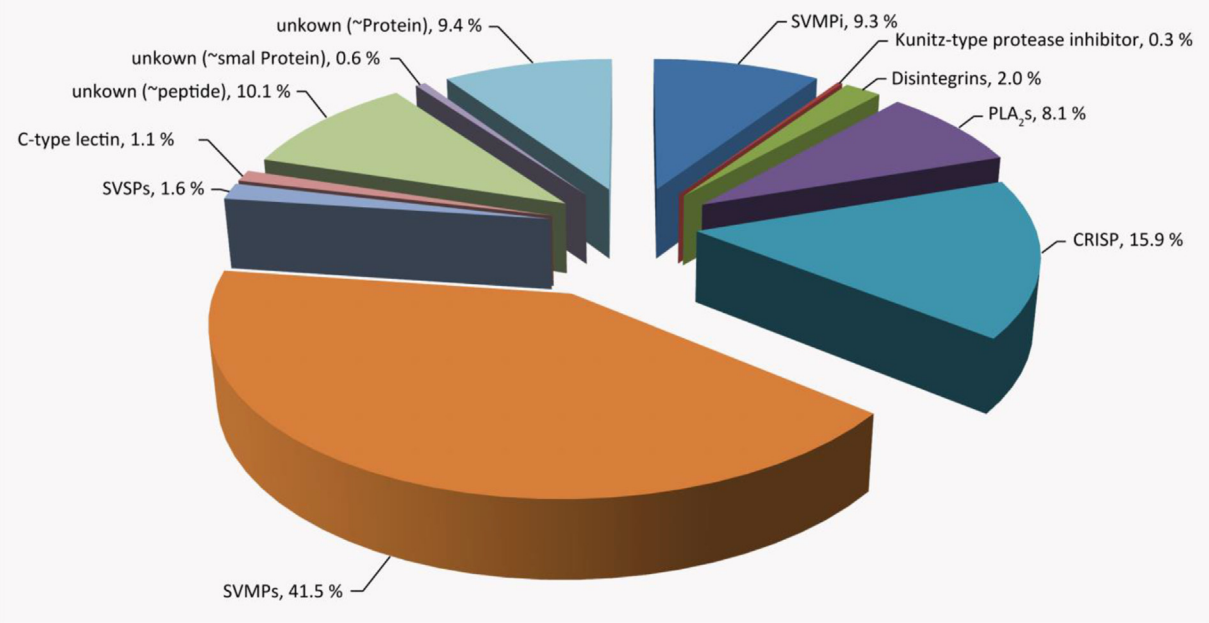

Fig. 4. Semi-quantitative venom composition of *Vipera anatolica*. The pie chart represents the relative occurrence of different toxin families. In our analysis we identified a snake venom metalloprotease inhibitor (SVMPi); a Kunitz-type protease inhibitor; disintegrins; Phospholipases of type A2 (PLA_2s); a CRISP, cysteine-rich secretory proteins; SVMPs, snake venom metalloproteinase; a SVSP, snake venom serine proteases, and a C-type lectin.

Kunitz-type protease inhibitor (0.3%).

As the first line of quantification relies on the UV signal from the HPLC run, the molar extinction coefficient ε of the peptides plays a crucial role for the peak areas of the toxins. Thus, our quantification is based on the simple assumption that these compound-specific values are nearly equal. This indeed might be the case for compounds of the same protein family but is rather unlikely for the comparison of peptides with high molecular mass proteins. Especially the concentration of the SVMPi, containing a Trp residue at the C-terminus, might be overestimated as ε-value is most likely higher than of the other compounds. Thus the venom composition has to be considered as semi-quantitative.

3.4. Medical implications

In comparison with other viper species, effects through envenomation caused by *V. anatolica* are generally low and not life threatening. After two accidental bite cases with *V. anatolica* during our field studies, the subjects (healthy, 51 and 28 years old, both male) reported only local pain and itch at the bitten area without any other complications. Similar symptoms were reported by Krecsak et al. (Krecsak et al., 2011) for the closely related small-sized insectivorous snakes viper *Vipera* (*Acridophaga*) *ursinii*. On the other hand, in a case study about accidents with another viper species to be found in Turkey, the blunt-nosed viper, *Macrovipera lebetina obtusa*, strong clinical symptoms and physiological damage were reported (Göçmen et al., 2006b). The difference in the toxicity can be explained by the bigger size and higher amount of venom injected by *M. lebetina obtusa*, but also the higher abundance of PLA_2 (~34% vs. ~ 8% *V. anatolica*) (Igci and Demiralp, 2012) might be a reason for the stronger necrotic effects as well as swelling-associated symptoms.

3.5. Cytotoxicity screening

To assess the potential of the toxins against cancer cells, we assessed the cytotoxicity of crude venom against the following cell lines: CACO-2, human colon carcinoma epithelial cells; MCF-7, human breast adenocarcinoma epithelial cells; U87MG, human glioblastoma-astrocytoma epithelial-like cells; PC3, human prostate epithelial cells; HeLa, human cervical epithelial carcinoma cells; MPanc-96, human pancreatic fibroblast cells; A549, human lung epithelial cells; HEK293, human embryonic epithelial kidney cell; Vero, African green monkey fibroblast-like kidney cells. We therefore performed initial cytotoxicity assays by means of an MTT assay which measures the mitochondrial reductase activity of cells and therefore is a measure for viability of cells. In Fig. 5 it can be seen that crude venom of the Anatolian Meadow Viper inhibits cell viability in a dose-dependent manner. The IC_{50} values for all affected cell lines are shown in Table 2. MCF-7, MPanc-96 and A549 were herby the most resistant cell lines against all venom doses tested (IC_{50} > 50 μg/mL), while PC3, HEK293, CACO-2, Vero and HeLa cells were only moderately affected (IC_{50} ~ 4.9; 5.5 and 7.2; 11.7 and 13.2 μg/mL respectively). The highest activity was observed against brain cancer cells (U87MG) with an IC_{50} value of ~0.8 μg/mL, which is more than one order of magnitude lower than against the non-cancerogenous cell lines (HEK293 and Vero). Remarkably, the crude venom cytotoxic effects on glioblastoma cells as well as the selectivity to cancer cells are notably higher than of the plant-derived sesquiterpene lactone parthenolide, a promising candidate in anti-cancer research. Microphotography of treated cells (shown in the supplemental information) showed similar results in comparison to the MTT assay. Untreated cells were homogeneously distributed in the culture plates showing typical morphological characteristics. Whereas morphological changes were observed after treatment with crude venom for 48 h varied depending on the origin of the cell lines. Increasing venom concentrations resulted in a higher number of rounded, detached cells, elevated mobility and distribution of cells on the surface, multicellular aggregate formation and growth inhibition compared to untreated cells. In addition, cell disorganization and large areas without cells were observed with increasing venom concentrations.

Because the amount of fractionated venom generally were very

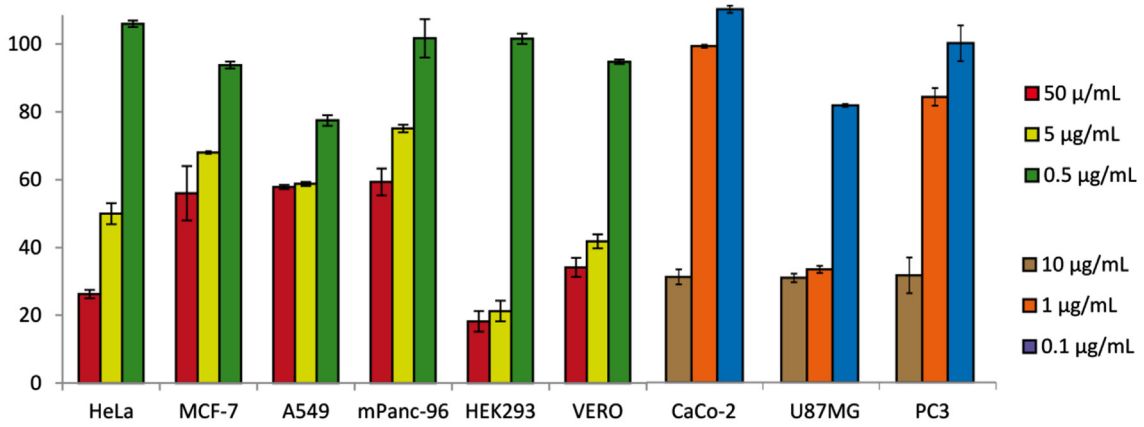

Fig. 5. Viability of cancer and non-cancerous cell lines after crude venom treatment for 48 h. Cell viability was determined by MTT assay, control was exposed to vehicle only which was taken as 100% viability. CACO-2, human colon carcinoma epithelial cells; MCF-7, human breast denocarcinoma epithelial cells; U87MG, human glioblastoma-astrocytoma epithelial-like cells; PC3, human prostate epithelial cells; HeLa, human cervical epithelial carcinoma cells; MPanc-96, human pancreatic fibroblast cells; A549, human lung epithelial cells; HEK293, human embryonic epithelial kidney cell; Vero, African green monkey fibroblast-like kidney cells.

Table 2
IC_{50} values of *V. anatolica* crude venom and Parthenolide treated cell lines. CACO-2, human colon carcinoma epithelial cells; MCF-7, human breast adenocarcinoma epithelial cells; U87MG, human glioblastoma-astrocytoma epithelial-like cells; PC3, human prostate epithelial cells; HeLa, human cervical epithelial carcinoma cells; MPanc-96, human pancreatic fibroblast cells; A549, human lung epithelial cells; HEK293, human embryonic epithelial kidney cell; Vero, African green monkey fibroblast-like kidney cells.

Cell lines	*V. anatolica venom* [µg/mL]	Parthenolide [µg/mL]
CACO-2	7.21 ± 0.12	0.69 ± 0.08
MCF-7	>50	1.17 ± 0.06
U87MG	0.75 ± 0.010	1.93 ± 0.05
PC3	4.85 ± 0.18	1.28 ± 0.07
HeLa	13.15 ± 0.13	3.33 ± 0.12
MPanc-96	>50	0.58 ± 0.02
A549	>50	1.66 ± 0.09
HEK293	5.52 ± 0.21	0.63 ± 0.04
Vero	11.65 ± 0.16	2.58 ± 0.10

low (0.04–9.03 µg) the isolated toxins were only tested against the most sensitive cell line (U87MG) of the crude venom cytotoxicity results. The results for peak 11 collected by semipreparative HPLC are shown in Fig. 6 (The results of the other fractions can be found in the supplemental information). Hereby, the only active fraction (Peak 11), containing a dimeric disintegrin, had a significant cytotoxic effect on glioblastoma cells with an IC_{50} value of 0.51 ± 0.04 µg/ml which is slightly better than the IC_{50} of crude venom (0.75 µg/mL). However comparing the fractions activity with the activity of parthenolide we found a twofold higher cytotoxicity. If the molecular mass ratio between parthenolide and disintegrin (248 Da: ~14.0 kDa) are considered, then the molar activity of peak 11 (~36 nM) is around 100 times higher than that of parthenolide. In comparison to the cytotoxic effects of recombinant disintegrins, r-viridistatin 2 and r-mojastin 1, peak 11 was significantly more active against BXPC-3 pancreatic cells with IC_{50} value of 10.6 and 8.7 µM(Lucena et al., 2015). The disintegrin colombistatin, isolated from *Bothrops colombiensis*, on the other hand showed similar IC_{50} against T24 and SK-Mel-28 cells (4.4 µM and 33 nM) (Sanchez et al., 2009).

Cytotoxic activity of disintegrins against glioblastoma, has been described to be caused by targeting specific integrins ultimately resulting in decrease of tumor growth, affecting invasion and migration of tumor cells in carcinogenesis (Calvete et al., 2005; Macedo et al., 2015). Cell adhesion and migration are important stages in metastasis development in which integrins, a class of

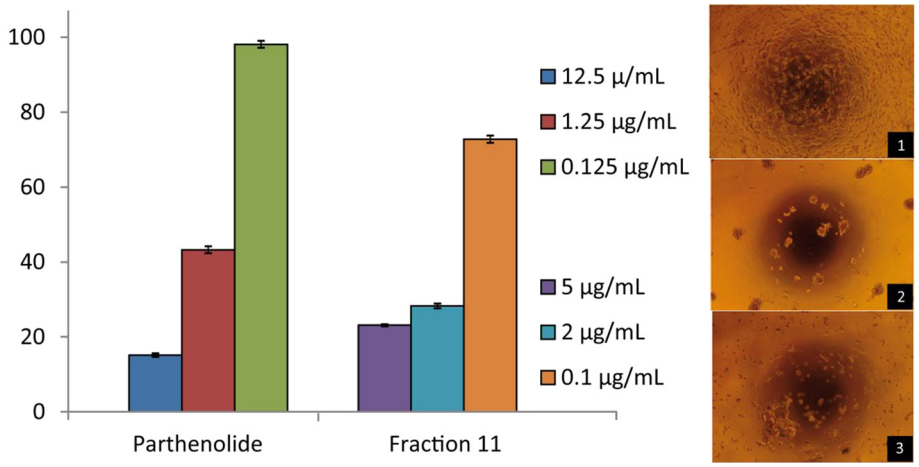

Fig. 6. A: Viability of U87MG cells after treatment with fraction 11 for 48 h. Cell viability was determined in an MTT assay, normalized to a control (100% viability). B: Effect of the isolated disintegrin on U87MG cells. Cells were treated with fractionated venom (fraction 11) for 48 h at 37 °C. 1: untreated, 2: treated with peak 11 2 µg/ml, 3: treated with parthenolide, 1.25 µg/ml.

receptors that modulate cell attachment, cell–cell and cell-extracellular matrix interactions, are significantly involved (Macedo et al., 2015). Here, the molecular target could be the RGD (Arg-Gly-Asp)-binding α5β1 and αvβ3 integrins which are known to be important for single cell migration and highly expressed in U87MG cells (Maurer et al., 2009; Ray et al., 2014). Thus, snake venom and particularly the dimeric disintegrin isolated from *V. anatolica* might have a promising potential as therapeutic anti-cancer agents.

To further investigate the anti-cancer properties of the herein described disintegrin (peak 11) full protein sequencing is needed in order to establish its primary sequence. Due to the low abundance and difficulties obtaining sufficient amounts of venom, the best approach would be cDNA cloning of the venom gland mRNA, which would enable us to heterologously express and produce the toxin. A transcriptomic analysis of the venom gland tissue would also facilitate the interpretation of mass spectra and thus allow us to obtain deeper insights into the complexity of the Anatolian Meadow Viper venom.

4. Conclusions

In conclusion, this study is an important step towards a complete profiling of the venom of *Vipera anatolica*. Based on a minimal amount of venom, we applied a combination of top-down and bottom-up mass spectrometry, which enabled us to detect ~110 venom components of which 100 different molecular masses were detected by intact protein mass spectrometry and ~10 exclusively by SDS-PAGE. Out of 36 isolated fractions we could identify 8 different toxin families. By means of MS/MS *de novo* sequencing of tryptic peptides as well as of intact proteins and peptides we could identify a snake venom metalloprotease inhibitor; a Kunitz-type protease inhibitor; disintegrins; phospholipases A_2; cysteine-rich secretory proteins; snake venom metalloproteinase; snake venom serine proteases, and a C-type lectin. The application of top-down mass spectrometry facilitated the detection of considerably more venom components as we were able to detect by a bottom-up approach. Even though a full protein identification by top-down MS/MS remains a challenging task for high molecular mass venom compounds, e.g. for metalloproteases, the mass profiling of intact toxins significantly improves the characterization of the complexity of snake venoms.

During our search for pharmacological interesting compounds we identified a dimeric disintegrin which showed remarkable cytotoxic activity against U87MG cells, influencing the cell shape, survival and proliferation and migration, which will be further assessed in our ongoing studies.

Acknowledgment

This study was supported by the Deutsche Forschungsgemeinschaft (DFG), Cluster of Excellence Unifying Concepts in Catalysis (UniCat) and by the Scientific and Technical Research Council of Turkey (TÜBİTAK) under Grant 111T338. We thank Dr. Rashed Al Toma and Eric van Herwerden (TU Berlin) for helpful discussion on the manuscript as well as Mert Karış, M. Anıl Oğuz and Volkan Eroğlu (Ege University, İzmir) for field assistances. We also thank to AREL (Ege University School of Medicine Research and Education Laboratory) for the permission to use their laboratory.

Appendix A. Supplementary data

Supplementary data related to this article can be found at http://dx.doi.org/10.1016/j.toxicon.2015.09.013.

References

Altschul, S.F., Gish, W., Miller, W., Myers, E.W., Lipman, D.J., 1990. Basic local alignment search tool. J. Mol. Biol. 215, 403–410.
Böhme, W., Joger, U., 1983. Eine neue art des Vipera berus-Komplexes aus der Türkei. Amphib. Reptil.s 4, 265–271.
Bradford, M.M., 1976. A rapid and sensitive method for the quantitation of microgram quantities of protein utilizing the principle of protein-dye binding. Anal. Biochem. 72, 248–254.
Brahma, R.K., McCleary, R.J., Kini, R.M., Doley, R., 2015. Venom gland transcriptomics for identifying, cataloging, and characterizing venom proteins in snakes. Toxicon 93, 1–10.
Calderon, L.A., Sobrinho, J.C., Zaqueo, K.D., de Moura, A.A., Grabner, A.N., Mazzi, M.V., Marcussi, S., Nomizo, A., Fernandes, C.F., Zuliani, J.P., Carvalho, B.M., da Silva, S.L., Stabeli, R.G., Soares, A.M., 2014. Antitumoral activity of snake venom proteins: new trends in cancer therapy. Biomed. Res. Int. 2014, 203639.
Calvete, J.J., 2013. Snake venomics: from the inventory of toxins to biology. Toxicon 75, 44–62.
Calvete, J.J., 2014. Next-generation snake venomics: protein-locus resolution through venom proteome decomplexation. Expert Rev. Proteom. 11, 315–329.
Calvete, J.J., Marcinkiewicz, C., Monleon, D., Esteve, V., Celda, B., Juarez, P., Sanz, L., 2005. Snake venom disintegrins: evolution of structure and function. Toxicon 45, 1063–1074.
Casewell, N.R., Wagstaff, S.C., Wuster, W., Cook, D.A., Bolton, F.M., King, S.I., Pla, D., Sanz, L., Calvete, J.J., Harrison, R.A., 2014. Medically important differences in snake venom composition are dictated by distinct postgenomic mechanisms. Proc. Natl. Acad. Sci. U. S. A. 111, 9205–9210.
Chippaux, J.-P., 2006. Clinic and Treatment of Envenomations. Krieger Publishing Company.
Ferreira, S.H., 1965. A bradykinin-potentiating factor (Bpf) present in the venom of Bothrops Jararca. Br. J. Pharmacol. Chemother. 24, 163–169.
Fry, B., 2015. Venomous Reptiles and Their Toxins: Evolution, Pathophysiology and Biodiscovery. Oxford University Press.
Ge, Y., Lawhorn, B.G., ElNaggar, M., Strauss, E., Park, J.H., Begley, T.P., McLafferty, F.W., 2002. Top down characterization of larger proteins (45 kDa) by electron capture dissociation mass spectrometry. J. Am. Chem. Soc. 124, 672–678.
Göçmen, B., Arikan, H., Mermer, A., Langerwerf, B., Bahar, H., 2006a. Morphological, hemipenial and venom electrophoresis comparisons of the Levantine Viper, Macrovipera lebetina (Linnaeus, 1758), from Cyprus and Southern Anatolia. Turk. J. Zool. 30, 225–234.
Göçmen, B., Arikan, H., Ozbel, Y., Mermer, A., Çiçek, K., 2006b. Clinical, physiological and serological observations of a human following a venomous bite by Macrovipera lebetina lebetina (Reptilia: Serpentes). Turk. Parazitol. Derg. 30 (2), 158–162.
Göçmen, B., Mulder, J., Kariş, M., Oğuz, M.A., 2014. The poorly known Anatolian Meadow Viper, Vipera anatolica: new morphological and ecological data. Herpetol. Romanica 8, 1–10.
Goncalves-Machado, L., Pla, D., Sanz, L., Jorge, R.J., Leitao-De-Araujo, M., Alves, M.L., Alvares, D.J., De Miranda, J., Nowatzki, J., de Morais-Zani, K., Fernandes, W., Tanaka-Azevedo, A.M., Fernandez, J., Zingali, R.B., Gutierrez, J.M., Correa-Netto, C., Calvete, J.J., 2015. Combined venomics, venom gland transcriptomics, bioactivities, and antivenomics of two Bothrops jararaca populations from geographic isolated regions within the Brazilian Atlantic rainforest. J. Proteom. http://dx.doi.org/10.1016/j.jprot.2015.04.029.
Igci, N., Demiralp, D.O., 2012. A preliminary investigation into the venom proteome of Macrovipera lebetina obtusa (Dwigubsky, 1832) from Southeastern Anatolia by MALDI-TOF mass spectrometry and comparison of venom protein profiles with Macrovipera lebetina lebetina (Linnaeus, 1758) from Cyprus by 2D-PAGE. Arch. Toxicol. 86, 441–451.
Kang, T.S., Georgieva, D., Genov, N., Murakami, M.T., Sinha, M., Kumar, R.P., Kaur, P., Kumar, S., Dey, S., Sharma, S., Vrielink, A., Betzel, C., Takeda, S., Arni, R.K., Singh, T.P., Kini, R.M., 2011. Enzymatic toxins from snake venom: structural characterization and mechanism of catalysis. Febs J. 278, 4544–4576.
King, G.F., 2011. Venoms as a platform for human drugs: translating toxins into therapeutics. Expert Opin. Biol. Ther. 11, 1469–1484.
Krecsak, L., Zacher, G., Malina, T., 2011. Clinical picture of envenoming with the Meadow Viper (Vipera (Acridophaga) ursinii). Clin. Toxicol. Phila 49, 13–20.
Lucena, S., Castro, R., Lundin, C., Hofstetter, A., Alaniz, A., Suntravat, M., Sanchez, E.E., 2015. Inhibition of pancreatic tumoral cells by snake venom disintegrins. Toxicon 93, 136–143.
Macedo, J.A., Castro, M.S., Fox, J.W., 2015. Disintegrins and their applications in cancer research and therapy. Curr. Protein Pept. Sci.
Maurer, G.D., Tritschler, I., Adams, B., Tabatabai, G., Wick, W., Stupp, R., Weller, M., 2009. Cilengitide modulates attachment and viability of human glioma cells, but not sensitivity to irradiation or temozolomide in vitro. Neuro Oncol. 11, 747–756.
McCleary, R.J., Kini, R.M., 2013. Non-enzymatic proteins from snake venoms: a gold mine of pharmacological tools and drug leads. Toxicon 62, 56–74.
Mosmann, T., 1983. Rapid colorimetric assay for cellular growth and survival: application to proliferation and cytotoxicity assays. J. Immunol. Methods 65, 55–63.
Munekiyo, S.M., Mackessy, S.P., 2005. Presence of peptide inhibitors in rattlesnake venoms and their effects on endogenous metalloproteases. Toxicon 45, 255–263.

Muth, T., Weilnbock, L., Rapp, E., Huber, C.G., Martens, L., Vaudel, M., Barsnes, H., 2014. DeNovoGUI: an open source graphical user interface for de novo sequencing of tandem mass spectra. J. Proteome Res. 13, 1143–1146.

Petras, D., Heiss, P., Sussmuth, R.D., Calvete, J.J., 2015. Venom proteomics of Indonesian King cobra, Ophiophagus hannah: integrating top-down and bottom-up approaches. J. Proteome Res.

Ray, A.M., Schaffner, F., Janouskova, H., Noulet, F., Rognan, D., Lelong-Rebel, I., Choulier, L., Blandin, A.F., Lehmann, M., Martin, S., Kapp, T., Neubauer, S., Rechenmacher, F., Kessler, H., Dontenwill, M., 2014. Single cell tracking assay reveals an opposite effect of selective small non-peptidic alpha5beta1 or alphavbeta3/beta5 integrin antagonists in U87MG glioma cells. Biochim. Biophys. Acta 1840, 2978–2987.

Reyes-Velasco, J., Card, D.C., Andrew, A.L., Shaney, K.J., Adams, R.H., Schield, D.R., Casewell, N.R., Mackessy, S.P., Castoe, T.A., 2015. Expression of venom gene homologs in diverse python tissues suggests a new model for the evolution of snake venom. Mol. Biol. Evol. 32, 173–183.

Rubin, B., Antonaccio, M.J., Horovitz, Z.P., 1978. Captopril (SQ 14,225) (D-3-mercapto-2-methylpropranoyl-L-proline): a novel orally active inhibitor of angiotensin-converting enzyme and antihypertensive agent. Prog. Cardiovasc. Dis. 21, 183–194.

Sanchez, E.E., Rodriguez-Acosta, A., Palomar, R., Lucena, S.E., Bashir, S., Soto, J.G., Perez, J.C., 2009. Colombistatin: a disintegrin isolated from the venom of the South American snake (Bothrops colombiensis) that effectively inhibits platelet aggregation and SK-Mel-28 cell adhesion. Arch. Toxicol. 83, 271–279.

Swenson, S., Costa, F., Minea, R., Sherwin, R.P., Ernst, W., Fujii, G., Yang, D., Markland Jr., F.S., 2004. Intravenous liposomal delivery of the snake venom disintegrin contortrostatin limits breast cancer progression. Mol. Cancer Ther. 3, 499–511.

Varol Tok, I.U., Murat, Sevinç, Wolfgang, Böhme, Pierre-André, Crochet, Ulrich, Joger, Yakup, Kaska, Yusuf, Kumlutaş, Uğur, Kaya, Aziz, Avci, Nazan, Üzüm, Can, Yeniyurt, Ferdi, Akarsu, 2015. Vipera anatolica – the IUCN Red list of threatened species. Version 2015.1. IUCN Red List Threat. Species.

Vetter, I., Davis, J.L., Rash, L.D., Anangi, R., Mobli, M., Alewood, P.F., Lewis, R.J., King, G.F., 2011. Venomics: a new paradigm for natural products-based drug discovery. Amino Acids 40, 15–28.

Vonk, F.J., Casewell, N.R., Henkel, C.V., Heimberg, A.M., Jansen, H.J., McCleary, R.J., Kerkkamp, H.M., Vos, R.A., Guerreiro, I., Calvete, J.J., Wuster, W., Woods, A.E., Logan, J.M., Harrison, R.A., Castoe, T.A., de Koning, A.P., Pollock, D.D., Yandell, M., Calderon, D., Renjifo, C., Currier, R.B., Salgado, D., Pla, D., Sanz, L., Hyder, A.S., Ribeiro, J.M., Arntzen, J.W., van den Thillart, G.E., Boetzer, M., Pirovano, W., Dirks, R.P., Spaink, H.P., Duboule, D., McGlinn, E., Kini, R.M., Richardson, M.K., 2013. The king cobra genome reveals dynamic gene evolution and adaptation in the snake venom system. Proc. Natl. Acad. Sci. U. S. A. 110, 20651–20656.

Wagstaff, S.C., Favreau, P., Cheneval, O., Laing, G.D., Wilkinson, M.C., Miller, R.L., Stocklin, R., Harrison, R.A., 2008. Molecular characterisation of endogenous snake venom metalloproteinase inhibitors. Biochem. Biophys. Res. Commun. 365, 650–656.

Woolf, C.J., 2013. Pain: morphine, metabolites, mambas, and mutations. Lancet Neurol. 12, 18–20.

Yalcin, H.T., Ozen, M.O., Gocmen, B., Nalbantsoy, A., 2014. Effect of Ottoman Viper (Montivipera xanthina (Gray, 1849)) venom on various Cancer cells and on Microorganisms. Cytotechnology 66, 87–94.

Zhang, Z., Marshall, A.G., 1998. A universal algorithm for fast and automated charge state deconvolution of electrospray mass-to-charge ratio spectra. J. Am. Soc. Mass Spectrom. 9, 225–233.

Zhou, Q., Sherwin, R.P., Parrish, C., Richters, V., Groshen, S.G., Tsao-Wei, D., Markland, F.S., 2000. Contortrostatin, a dimeric disintegrin from Agkistrodon contortrix contortrix, inhibits breast cancer progression. Breast Cancer Res. Treat. 61, 249–260.

Supplemental Information

Mass spectrometry guided venom profiling and bioactivity screening of the Anatolian Meadow Viper, *Vipera anatolica*

Bayram Göçmen[1*], Paul Heiss[2*], Daniel Petras[2], Ayse Nalbantsoy[3¥] and Roderich D. Süssmuth[2¥]

[1] Zoology Section, Department of Biology, Faculty of Science, Ege University, 35100 Bornova, Izmir, Turkey.

[2] Technical University of Berlin, Institute for Chemistry, Berlin, Germany

[3] Department of Bioengineering, Faculty of Engineering, Ege University, 35100 Bornova, Izmir, Turkey.

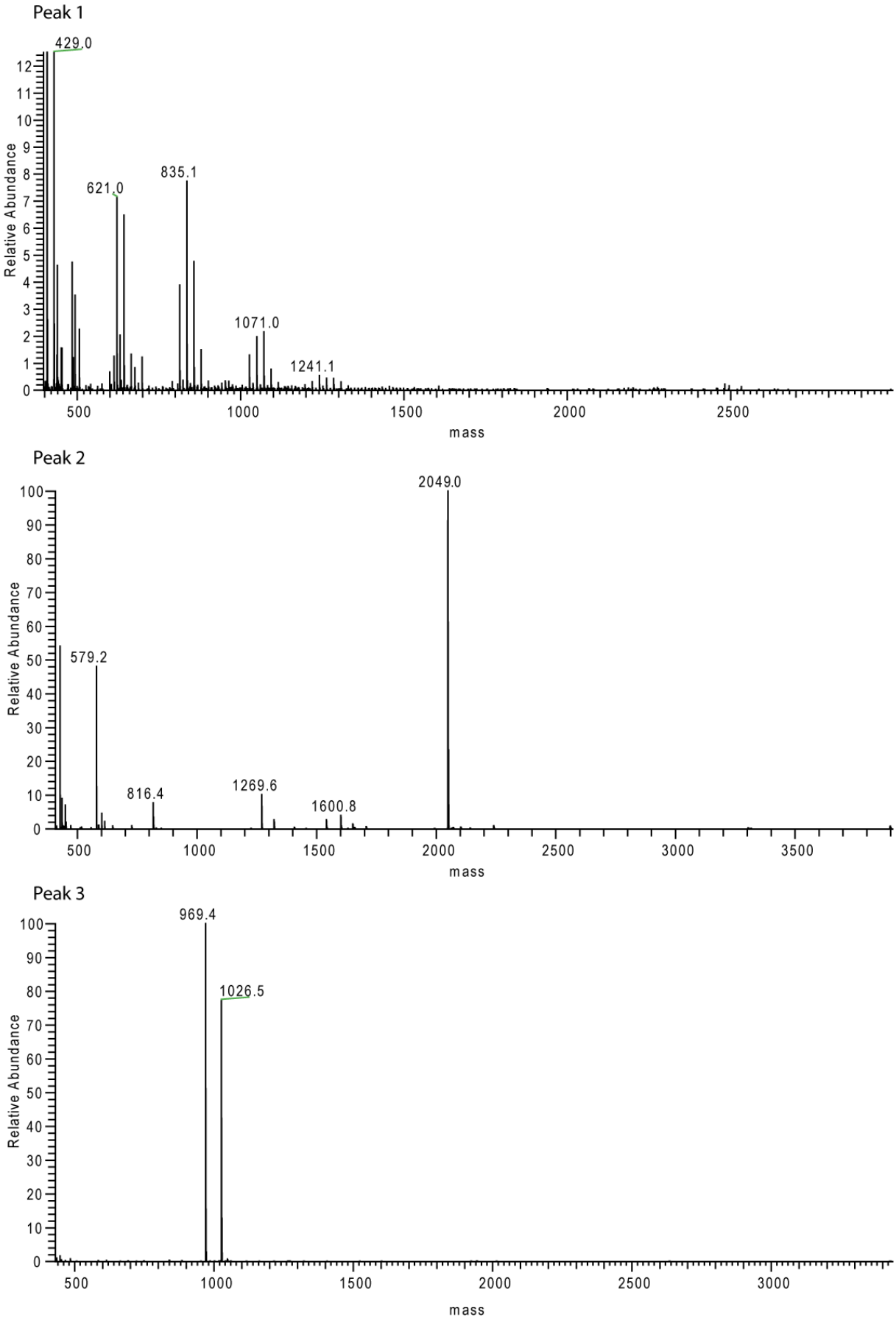

Supplemental Figure 1: Deconvoluted top-down mass spectra from *Vipera anatolica* (Peaks 1-34)

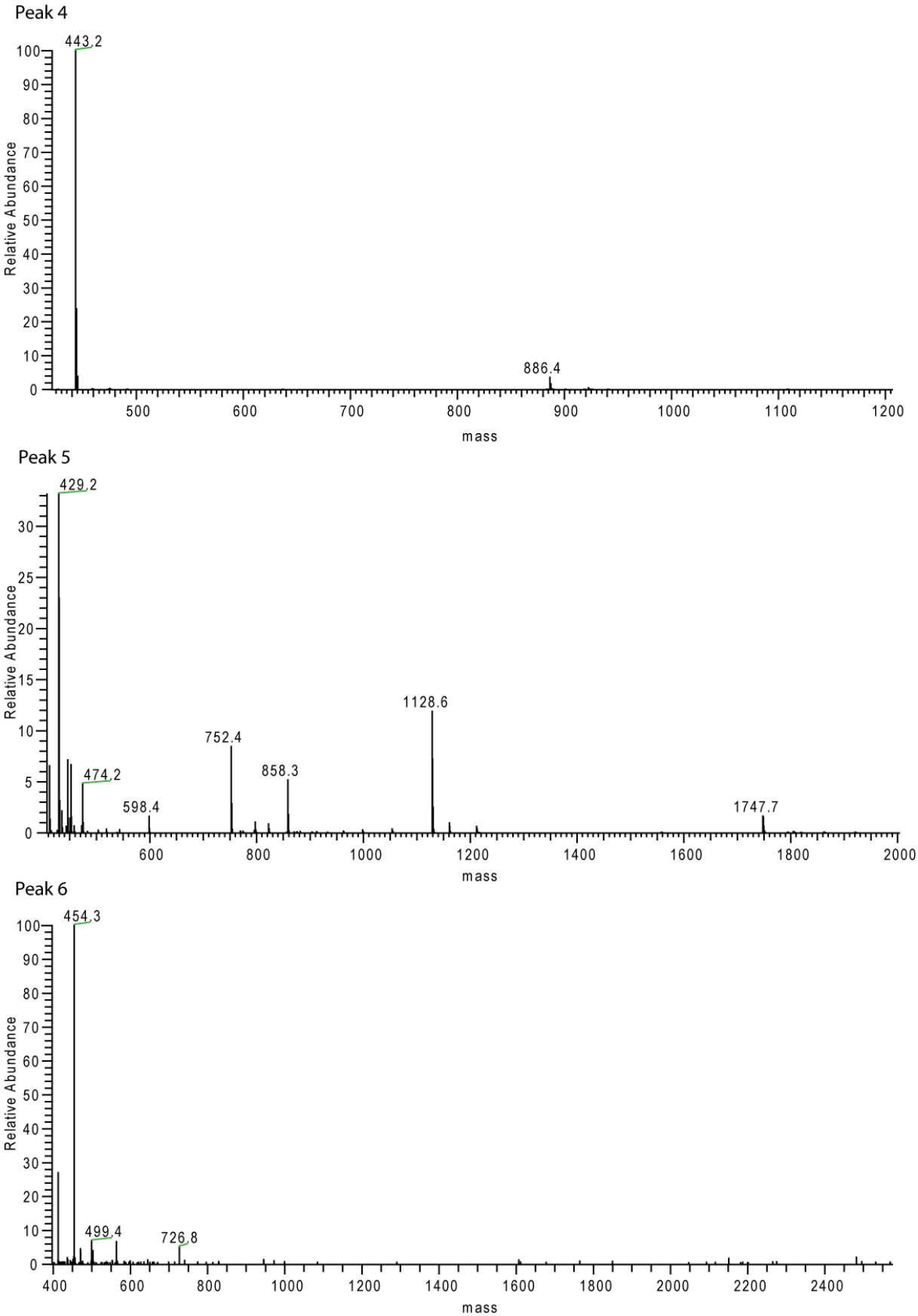

Supplemental Figure 1continued

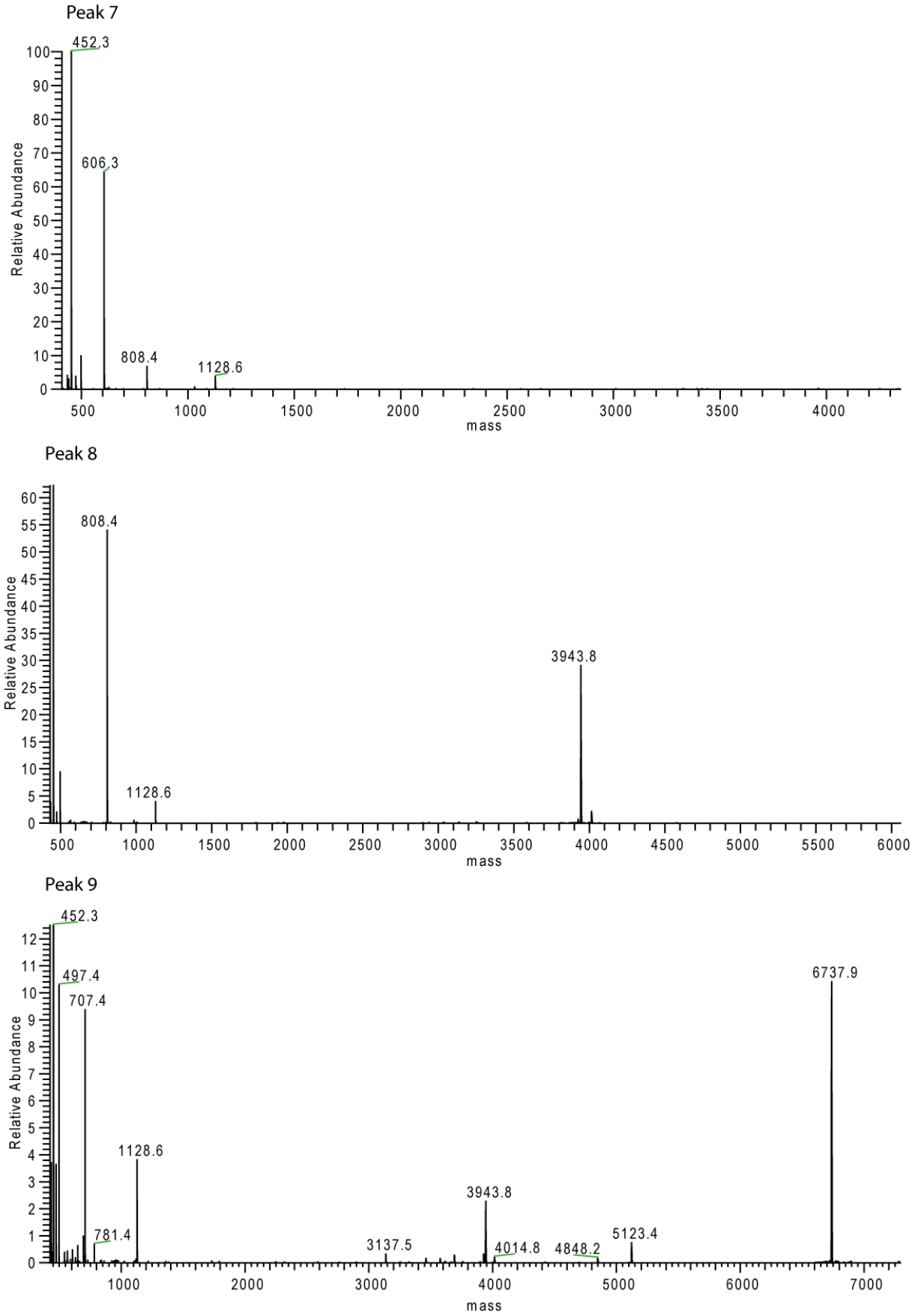

Supplemental Figure 1continued

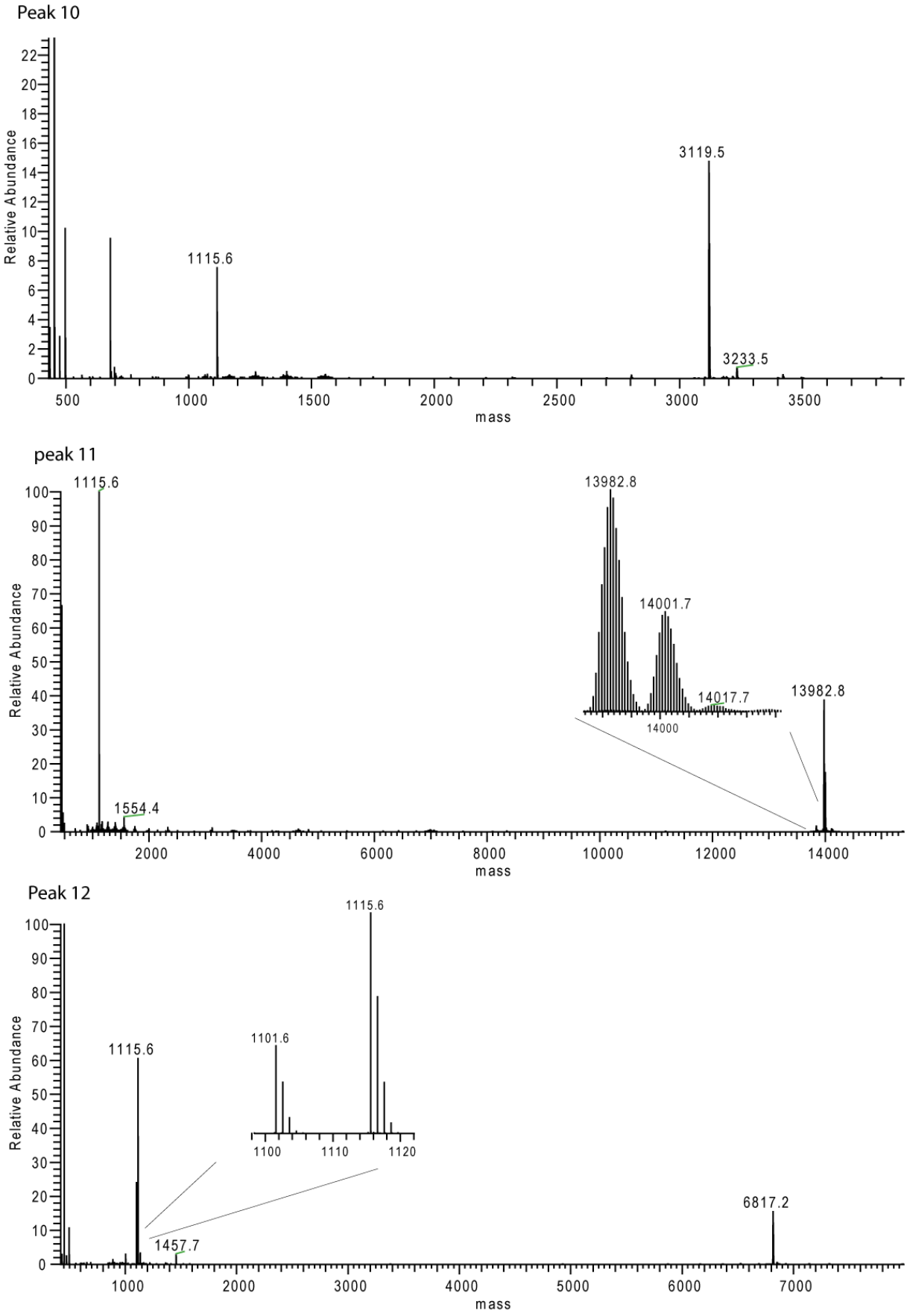

Supplemental Figure 1continued

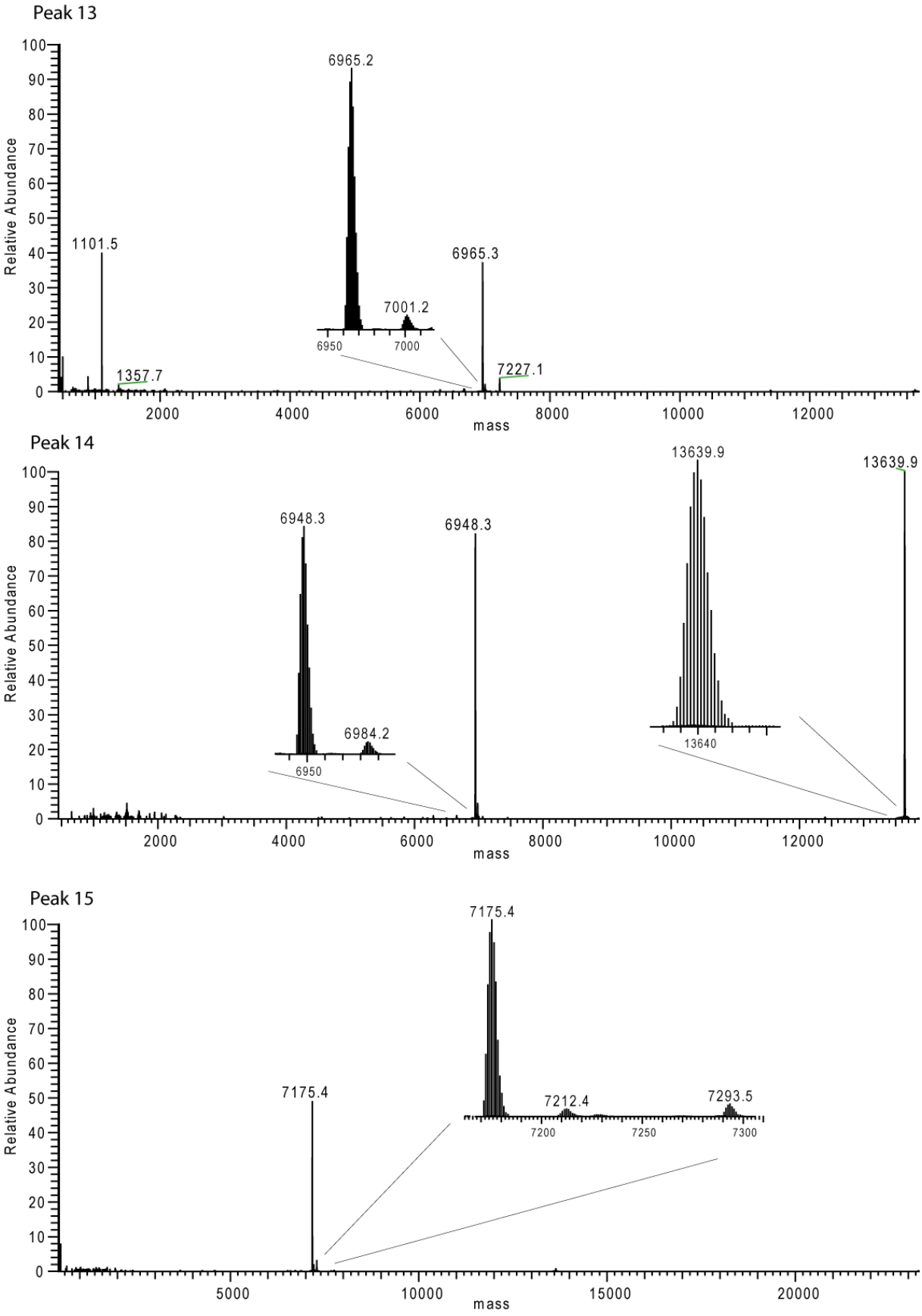

Supplemental Figure 1continued

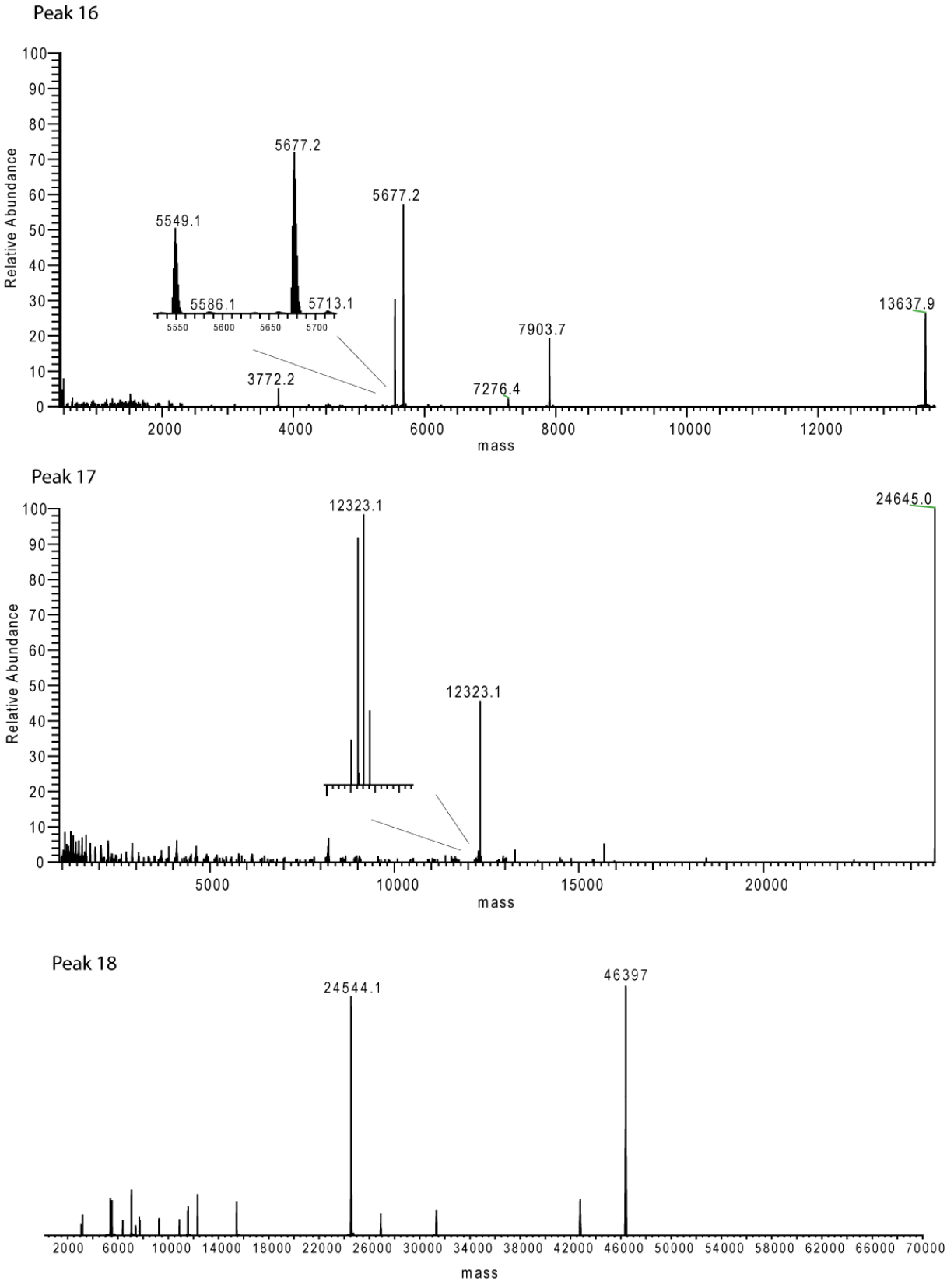

Supplemental Figure 1continued

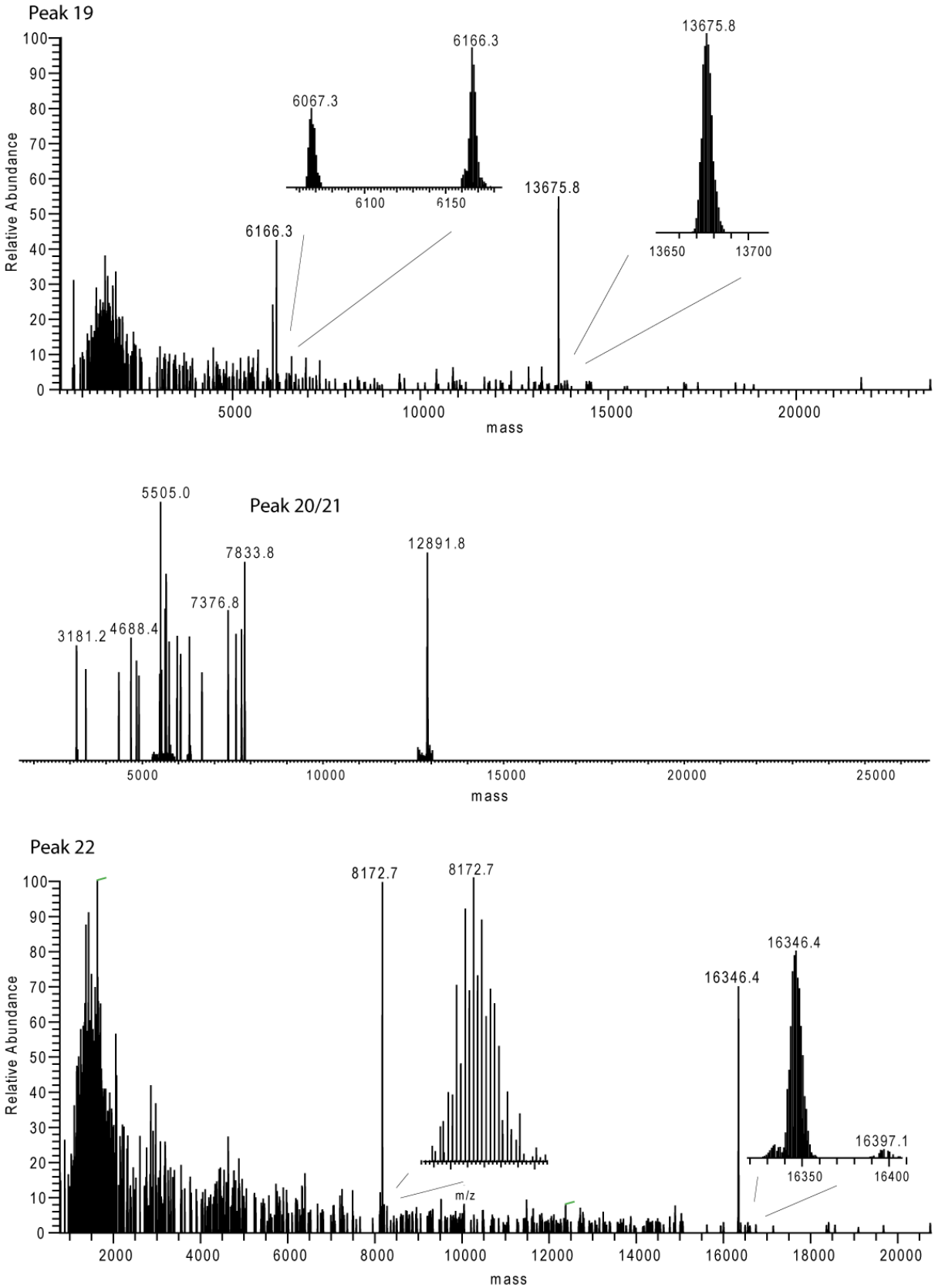

Supplemental Figure 1continued

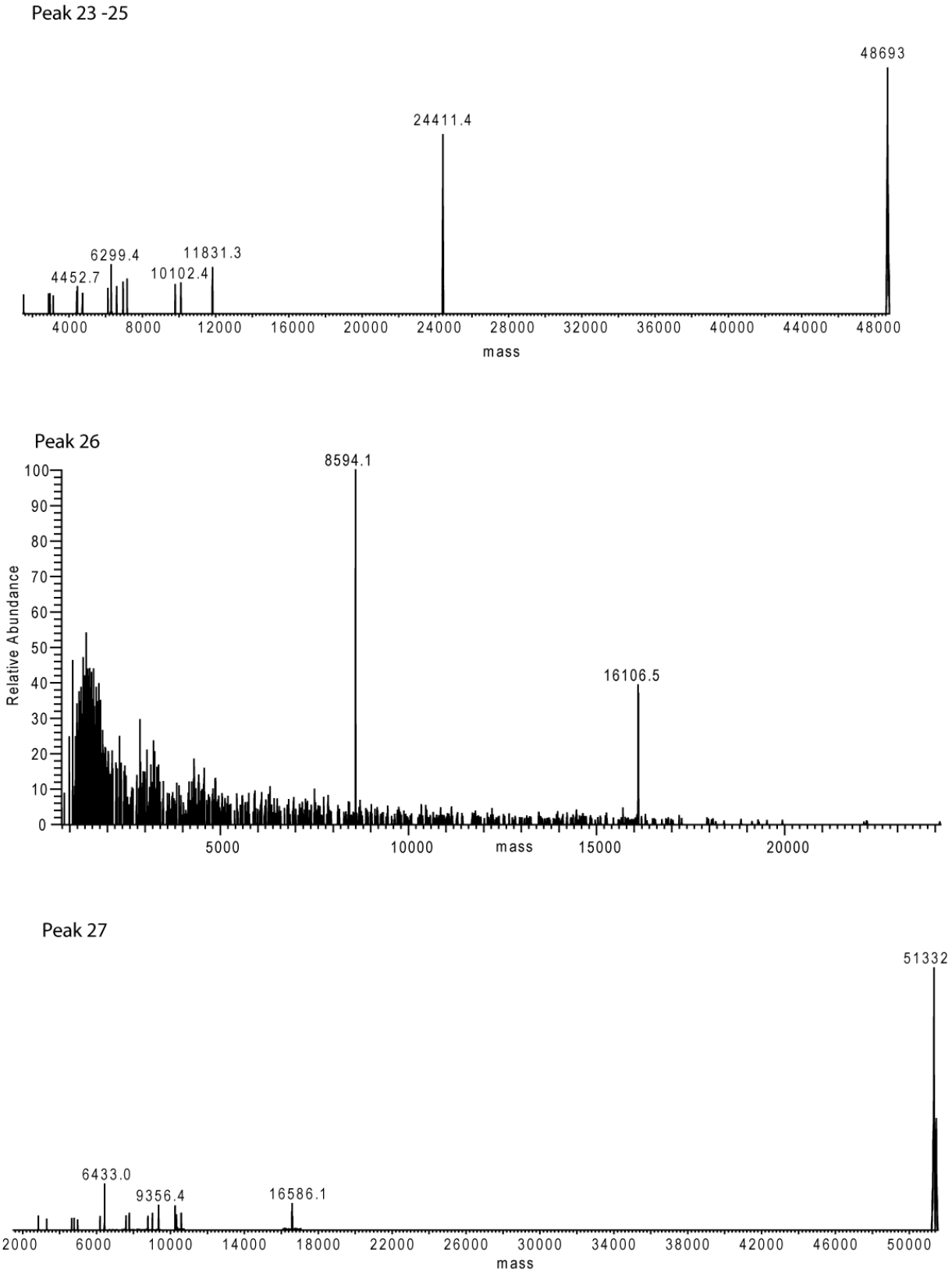

Supplemental Figure 1continued

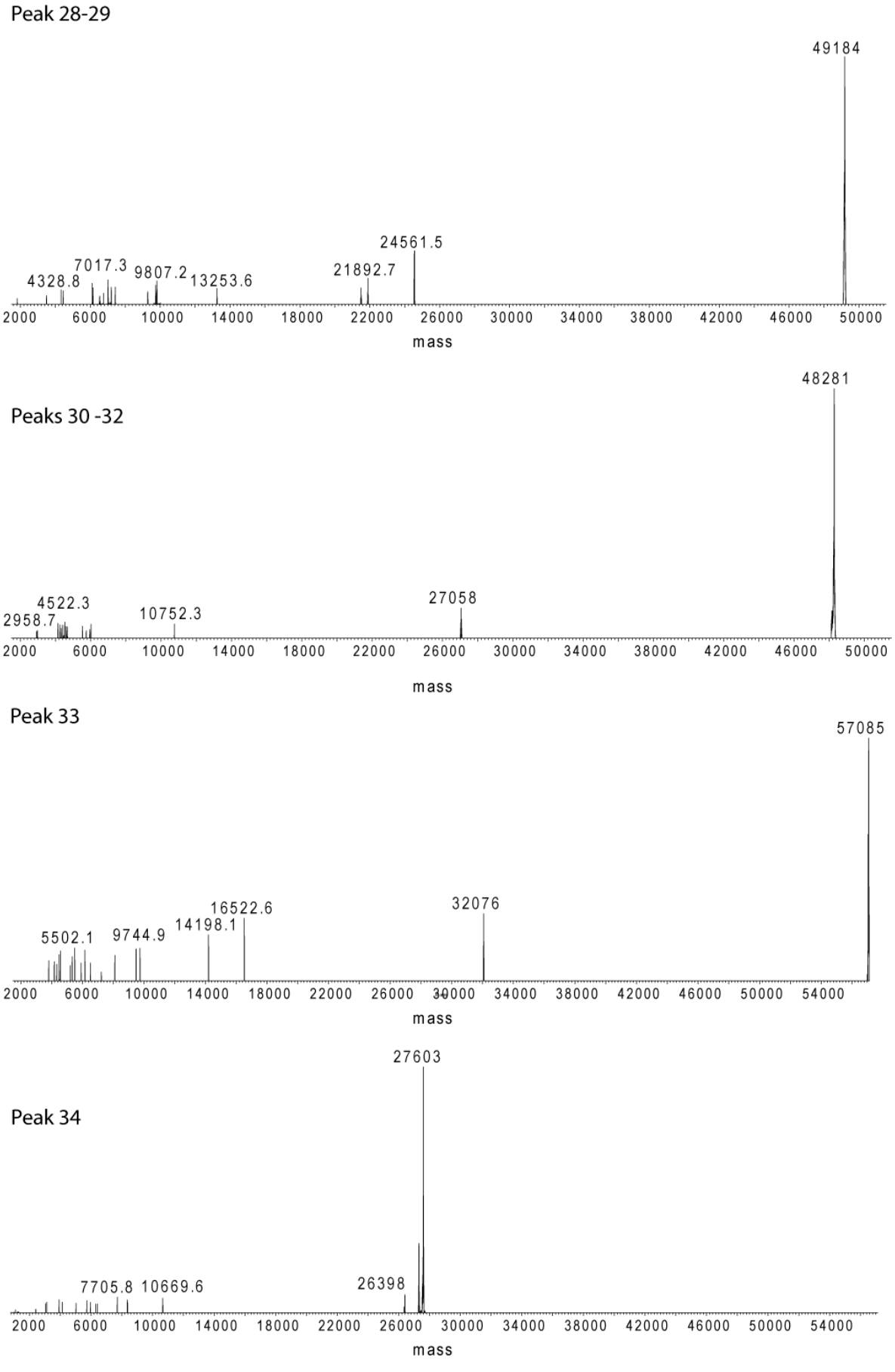

Supplemental Figure 1continued

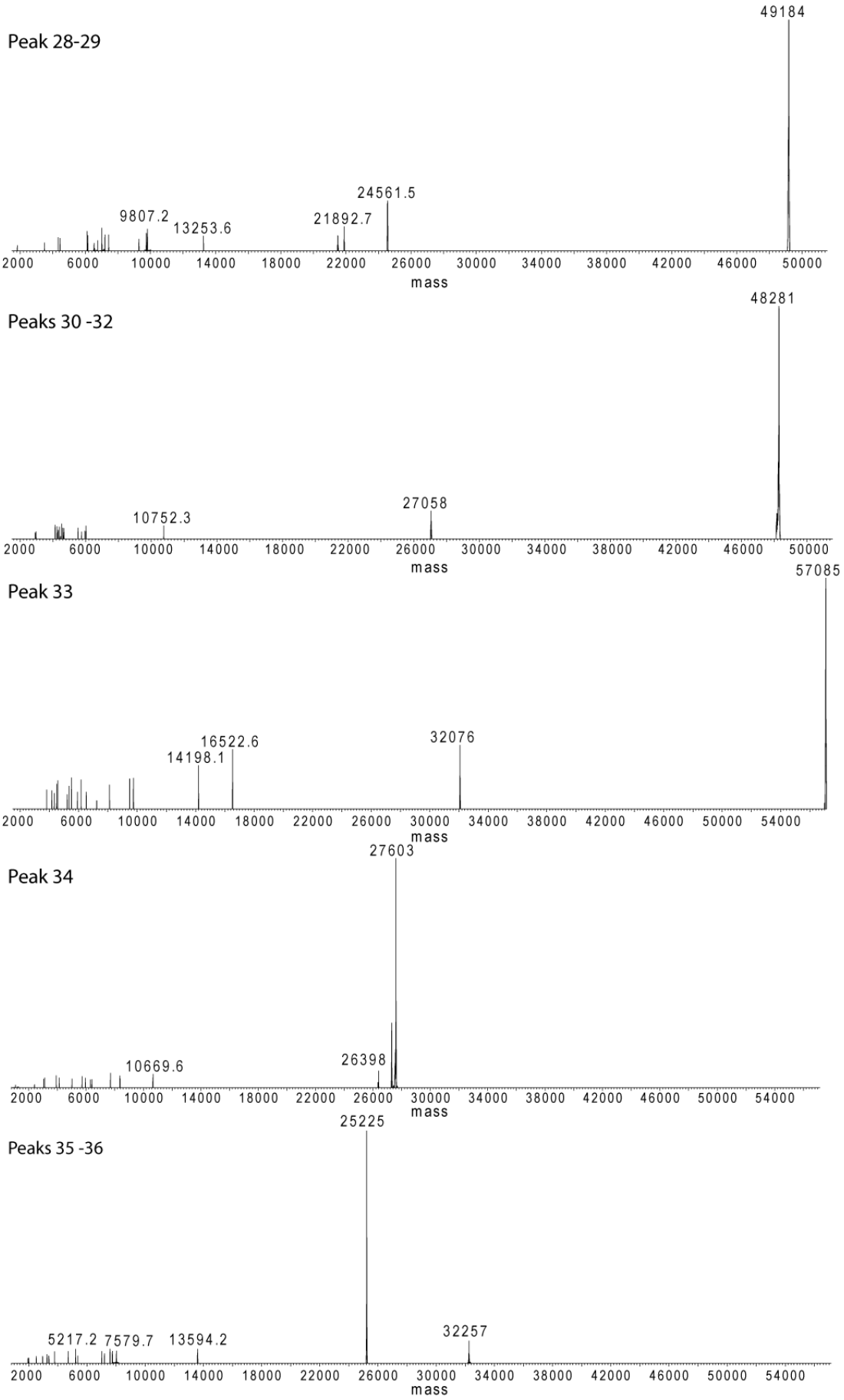

Supplemental Figure 1continued

Peak 4 - 443.2 Da

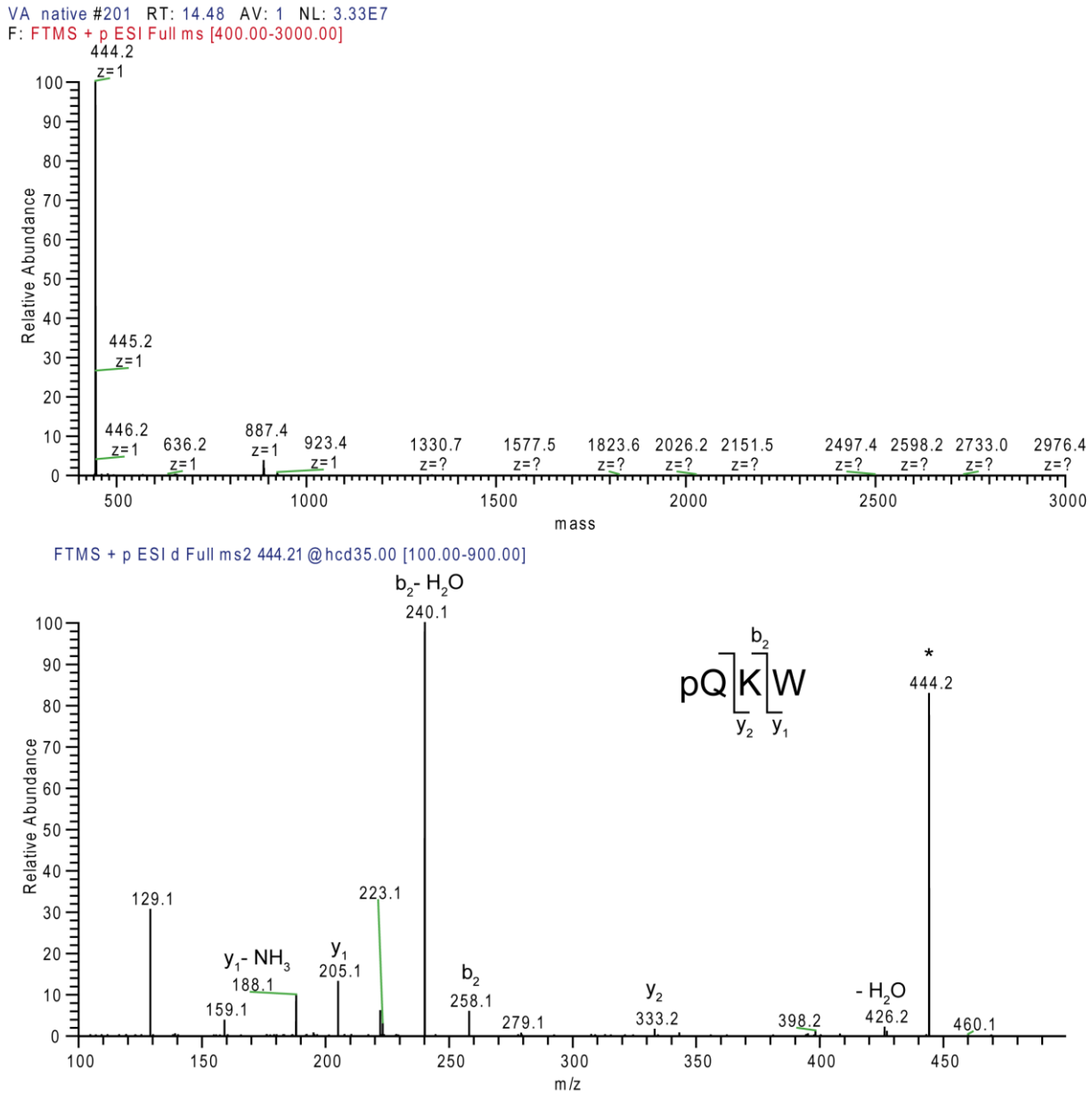

Supplemental Figure 2: MS and MSMS spectrum of the snake venom metalloprotease inhibitor.

Peak 14 - 5461.6 Da

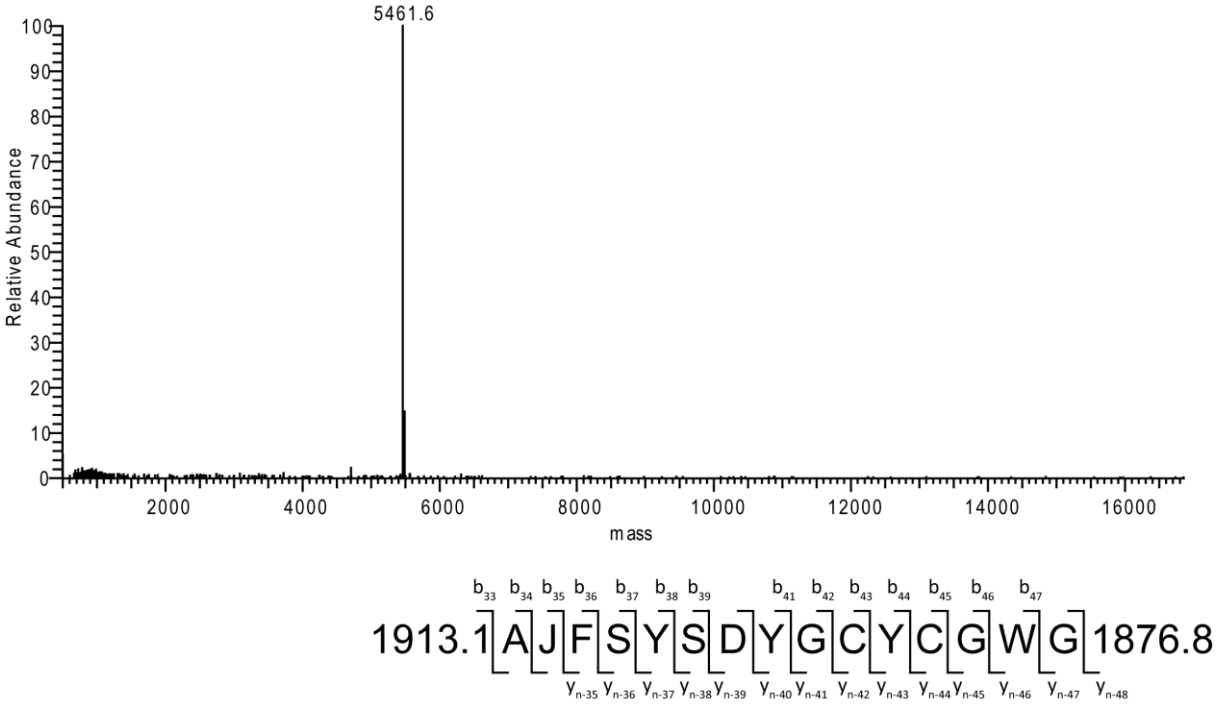

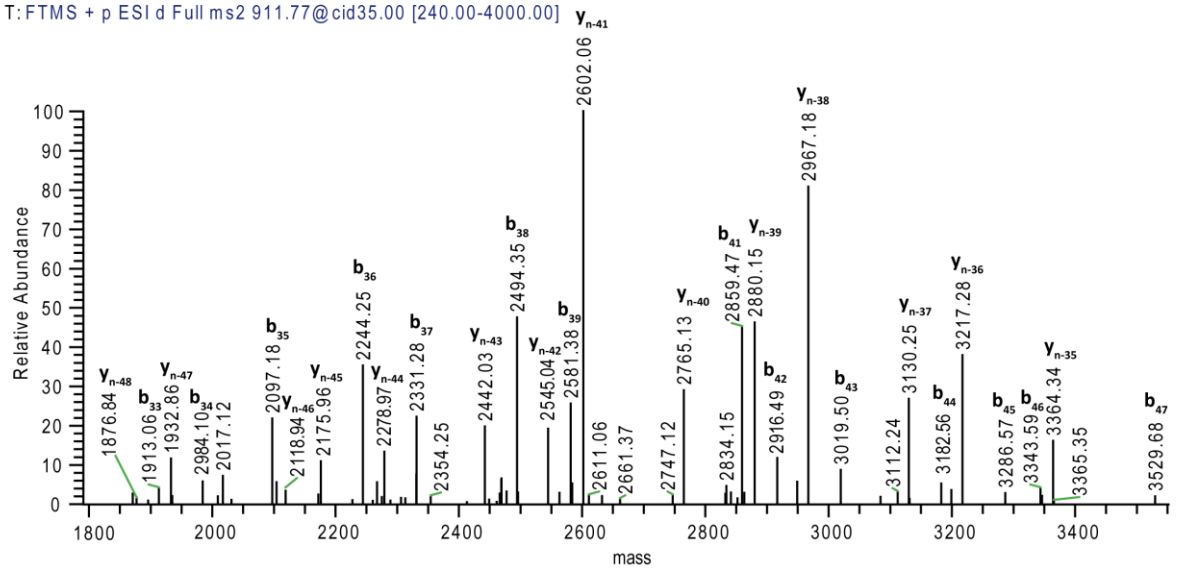

Supplemental Figure 3: Deconvoluted MS and MSMS spectrum (zoomed) of a PLA2 fragment.

Supplemental table 1: Cytotoxicity results of isolated fractions. IC_{50} values of *V. anatolica* fractions for U87MG cells following 48 h exposure are listed.

fractions number	IC_{50} [µg/mL]
Parthenolide	1.14±0.07
1	
2	-
3	-
4	-
5	-
6	-
8	-
11	0.51±0.04
14	-
17	-
18	-
19	-
20	-
21	-
23	-
25	-
26	-
27	-
28	-
29	-
30	-
31	-
32	-
33	-
34	-
35	-
36	-

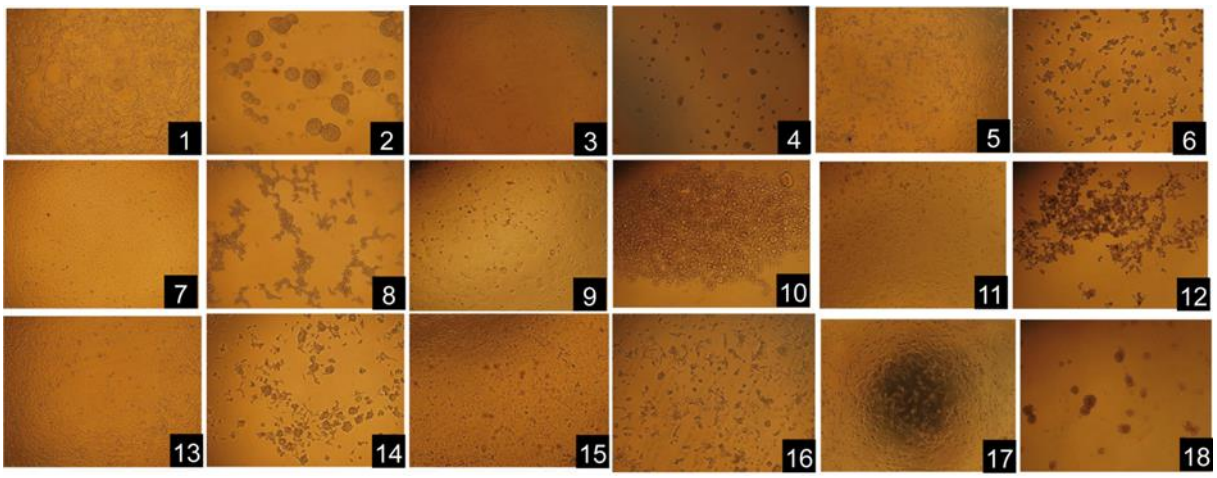

Supplemental Figure 2 Effect of crude venom on various cancer and non-cancerous cell lines. Cells were treated with crude venom for 48 h at 37° C. **1**: HEK293 untreated, **2:** HEK293, 10 µg/ml, **3:** Vero, untreated, **4:** Vero, 10 µg/ml, **5:** MPanc-96 untreated, **6:** MPanc-96, 10 µg/ml, **7:** A549, untreated, **8:** A549, 10 µg/ml, **9:** CACO-2, untreated, **10:** CACO-2, 10 µg/ml, **11:** PC-3, untreated, **12:** PC-3, 10 µg/ml, **13:** HeLa, untreated, **14:** HeLa, 10 µg/ml, **15:** MCF-7, untreated, **16:** MCF-7, 10 µg/ml, **17:** U87MG, untreated, **18:** U87MG, 10 µg/ml.